Editorial

〔Lab Med Int 2023; 2(3): 39〕

Can the absolute number of lymphocytes improve the overall quality of life of patients with HER2-negative recurrent breast cancer?

*†Kazuhito Ueda**

†Correspondence: Department of Medical Technology, Faculty of Health Sciences, Kansai University of Health Sciences, Kumatori-cho, Osaka 590-0482, Japan. E-mail: ueda@kansai.ac.jp

* Associate editor of Laboratory Medicine International; Department of Medical Technology, Faculty of Health Sciences, Kansai University of Health Sciences.

See article volume 2: 50-59

Mokuyasu et al. reported the effect of eribulin treatment on patients with HER2-negative recurrent breast cancer at their institution in their original research published in the journal Laboratory Medicine International titled "Absolute lymphocyte count is a prognostic factor in patients with HER2-negative recurrent breast cancer treated with eribulin". The authors reported the relationship between overall survival (OS), absolute lymphocyte count (bALC) and neutrophil/lymphocyte count ratio (NLR) in 114 HER2-negative breast cancer patients that were treated with eribulin[1].

Determining prognostic factors is useful as eribulin treatment is expensive, necessitating selection of patients for the treatment. Previous studies have reported that bALC and NLR are useful prognostic predictors in the eribulin-treated group[2]; however, the exact threshold values are yet to be established. In addition, simple indicators, that accurately predict prognosis prior to administration, can improve the overall quality of life of patients.

In the present study, the authors investigated the relationship between OS, the median values (bALC : 1,200/μL, NLR : 2) and threshold reported in previous studies[3] (bALC : 1,500/μL, NLR : 3). The results demonstrated that OS was significantly and specifically prolonged in the group with a bALC value above 1,200/μL, indicating its usefulness. No significant improvement was observed at bALC value of 1,500/μL and NLR : 2 and 3.

Regardless, previous reports[4] exist where bALC value of 1,000/μL has been found useful as a threshold and more detailed numerical values are possible if the cut-off value is not fixed and a significance difference test is performed, but analyzed as continuous values. A previous study has found a bALC value of 1.285/μL to be useful in a univariate analysis[5].

The increase in lymphocytes reflects enhanced anti-tumor immune activity, a factor in prolonging OS in the group with bALC greater than 1,200/μL. However, the present study did not consider the impact of treatments other than eribulin as well as the variation in optimal threshold between patient groups. Therefore, future studies with more patients are needed.

Reference

1) Mokuyasu S, Oshitanai R, Morioka T, et al. Absolute lymphocyte count is a prognostic predictor in patients with recurrent HER2-negative breast cancer treated with eribulin. Lab Med Int 2023; 2 (3) : 2023; 2 (3) : 50-9.

2) Kashiwagi S, Asano Y, Goto W, et al. Mesenchymal-epithelial transition and tumor vascular remodeling in eribulin chemotherapy for breast cancer. Anticancer Res 2018; 38 (1) : 401-10.

3) Morisaki T, Kashiwagi S, Asano Y, et al. Prediction of survival after eribulin chemotherapy for breast cancer by absolute lymphocyte counts and progression types. World J Surg Oncol 2021; 19 (1) : 324. doi: 10.1186/s12957-021-02441-w

4) Ueda Y, Makino Y, Hidaka H, et al. Analysis of prognostic factors considering absolute lymphocyte count of metastatic breast cancer patients with eribulin mesylate therapy - A retrospective study in a single institution. : Jpn J Cancer Chemother. Gan To Kagaku Ryoho 2022: 49 (11) : 1229-32.

5) Koyama Y, Kawai S, Uenaka N, et al. Absolute lymphocyte count, platelet-to-lymphocyte ratio, and overall survival in eribulin-treated HER2-negative metastatic breast cancer patients. : Cancer Diagn Progn 2021: 1 (5) : 435-41.

Editorial

〔Lab Med Int 2023; 2(3): 40-41〕

The important thing is not to stop questioning. Albert Einstein What have we learned from COVID-19 related studies?

†Tatsuo Shimosawa*

†Correspondence: Department of Clinical Laboratory, International University of Health and Welfare, 852 Hatakeda, Narita, Chiba 286-8520, Japan. E-mail: shimosawa-lab@iuhw.ac.jp

* Associate editor of Laboratory Medicine International: Department of Clinical Laboratory, International University of Health and Welfare.

Key Words

SARS-CoV-2, Antibody, Vaccination

See article volume 2: 60-66

The chaos has almost gone after 3 to 4 years struggle against SARS-CoV-2 pandemic. Looking back those days, we lost many valuables but at the same time, we obtained scientific progress that can be applied to not limited in infectious diseases but other medical fields. It is still fresh in memory that Drs. Katalin Karioko and Drew Weissman received the Nobel Prize in physiology or Medicine 2023 for their discoveries concerning nucleoside base modifications that enabled the development of effective mRNA vaccines against COVID-19. This advance will accelerate the research in developing mRNA vaccine against HIV or other infectious disease and cancer[1]. Thinking about clinical laboratory medicine, various methods to diagnose the infection were rapidly developed and widely used in regular clinical laboratories and well recognized by the patients. After developing the vaccines against COVID-19, a lot of research papers have been published in regards to the accuracy of measuring antibodies, time-course changes of antibodies, diagnostic values of measuring antibodies, class of immunoglobulin responses after natural infection and vaccination[2] or according to sex[3]. In the current issue, Kim and his colleagues reported the responses of neutralizing antibody against COVID-19 is different between naturally infected and vaccinated individuals[4]. They showed the titer of neutralizing antibody lasts at least three month after booster shot of vaccine. True neutralizing capacity of antibody is difficult to examine in routine laboratory without special equipment but Kim and his colleagues measured antibody against viral receptor biding domain which is reported to correspond to neutralizing capacity[5].

The current study provides us a clue to schedule of vaccination to maintain its effectiveness. We are facing several waves of influenza, COVID-19 or adenovirus infections all through the season. It is reported that response of neutralizing antibody after influenza vaccination varies by ages and host immune priming histories[6]. More detailed and large-scale investigations are required in character of neutralizing antibody after COVID-19 vaccination to establish the optimal vaccination schedule to prevent waves of infection.

References

1) Ankrah PK, Ilesanmi A, Akinyemi AO, Lasehinde V, Adurosakin OE, Ajayi OH. Clinical Analysis and Applications of mRNA Vaccines in Infectious Diseases and Cancer Treatment. Cureus 2023; 15(10): e46354. Epub 20231002. doi: 10.7759/cureus.46354. PubMed PMID: 37920621; PubMed Central PMCID: PMC10619190.

2) Fox T, Geppert J, Dinnes J, Scandrett K, Bigio J, Sulis G, et al. Antibody tests for identification of current and past infection with SARS-CoV-2. Cochrane Database Syst Rev 2022; 11(11): CD013652. Epub 20221117. doi: 10.1002/14651858. CD013652. pub2. PubMed PMID: 36394900; PubMed Central PMCID: PMC9671206.

3) Nakai M, Yokoyama D, Sato T, Sato R, Kojima C, Shimosawa T. Variation in antibody titers determined by Abbott and Roche Elecsys SARS-CoV-2 assays in vaccinated healthcare workers. Heliyon 2023; 9(6): e16547. Epub 20230522. doi: 10.1016/j.heliyon. 2023. e16547. PubMed PMID: 37235203; PubMed Central PMCID: PMC10201891.

4) Kim JH, Kikuchi R, Suzuki A, Watarai R, Goto K, Okumura Y, et al. Comparison of target antigen and immunoglobulin iso-

types in anti-SARS-CoV-2 antibodies from natural infection and vaccination. Lab Med Int 2023; 2(3): 60-6.

5) Noval MG, Kaczmarek ME, Koide A, Rodriguez-Rodriguez BA, Louie P, Tada T, et al. Antibody isotype diversity against SARS-CoV-2 is associated with differential serum neutralization capacities. Sci Rep 2021; 11(1): 5538. Epub 20210310. doi: 10.1038/s41598-021-84913-3. PubMed PMID: 33692390; PubMed Central PMCID: PMC7946906.

6) Liu F, Gross FL, Jefferson SN, Holiday C, Bai Y, Wang L, et al. Age-specific effects of vaccine egg adaptation and immune priming on A(H3N2) antibody responses following influenza vaccination. J Clin Invest 2021; 131(8). doi: 10.1172/JCI146138. PubMed PMID: 33690218; PubMed Central PMCID: PMC8262463.

Original

The coefficient of determination is affected by the attenuation coefficient in attenuation imaging

†Shingo Tanaka[*1,2,3], Noboru Ohba*[*2], Kiyoshi Abe*[*2], Yuka Tamoto*[*2], Kenji Yasui*[*2], Chihiro Kobayashi*[*2], Nagomi Saito*[*2], Koji Miyanishi*[*3], Satoshi Takahashi*[*1,2], Junji Kato*[*3]*

†Correspondence: Department of Infection Control and Laboratory Medicine, and Department of Medical Oncology, Sapporo Medical University School of Medicine, South-1, West-16, Sapporo 060-8543, Japan.
E-mail: stanaka@sapmed.ac.jp
Received November 17, 2022; accepted March 30, 2023
*1 Department of Infection Control and Laboratory Medicine, Sapporo Medical University School of Medicine, Sapporo, Japan.
*2 Division of Laboratory Medicine, Sapporo Medical University Hospital, Sapporo, Japan.
*3 Department of Medical Oncology, Sapporo Medical University School of Medicine, Sapporo, Japan.

ABSTRACT

Aims: Attenuation imaging (ATI) is a new ultrasonography method of evaluating hepatic steatosis. Attenuation coefficients (ACs) in the region of interest are measured using two-dimensional ultrasonography. ATI also displays the coefficient of determination (R^2) as an index of AC reliability. This study aimed to elucidate R^2 values in patients who underwent ATI in clinical practice and to determine factors that influence R^2 values.
Methods: This study included 749 patients who underwent ATI to evaluate hepatic steatosis at a single center. All abdominal ultrasound examinations were performed by one of the five experienced ultrasonographers. The AC and R^2 values were measured five times, and the median values were calculated. Multivariate analysis was conducted to identify factors affecting R^2 values.
Results: One hundred and nine (15%) patients showed R^2 values of < 0.80, of which 108 had non-fatty liver. Further, the R^2 value was strongly correlated with AC (correlation coefficient = 0.842). Uncomplicated diabetes (Odds ratio [OR], 2.68) and AC (< 0.60 dB/cm/MHz; OR, 72.76) were identified as independent factors associated with low R^2 values (< 0.80).
Conclusion: ATI in patients with non-fatty liver showed low R^2 values. Worldwide standardization of the ATI measurement method is urgently needed for consistent results.

〔Lab Med Int 2023; 2(3): 42-49〕

Key Words
abdominal ultrasonography, attenuation imaging, coefficient of determination, fatty liver, non-alcoholic fatty liver disease(NAFLD)

I. Introduction

Hepatic steatosis is a characteristic feature of non-alcoholic fatty liver disease (NAFLD), the most common cause of chronic liver disease (CLD) worldwide [1]. Hence, clinical evaluation of steatosis is important for the management of patients with CLD. Further, steatosis can also progress to non-alcoholic steatohepatitis (NASH) and clinically significant fibrosis in patients with NAFLD [2].

Abdominal ultrasonography (US) is the primary strategy for the diagnosis and assessment of fatty liver [3]; however, conventional B-mode US is operator dependent, and the diagnostic accuracy decreases in cases of mild steatosis [4]. To overcome these limitations, new methods for quantifying the transmitted US beam attenuation within the liver parenchyma have been developed [5]. The controlled attenuation parameter (CAP) of FibroScan,

the first US-based tool available for the quantification of hepatic steatosis, has been used in clinical practice with promising results [6)7)], although it is not an imaging modality and is associated with a high rate of measurement failure (0–24%) [8)].

Attenuation imaging (ATI) is a new ultrasound-based method for the assessment of hepatic steatosis [9)], which allows for positioning of the region of interest (ROI) for attenuation coefficient (AC) measurement using two-dimensional (2D) US imaging. ATI also displays the coefficient of determination (R^2) as an index of the AC reliability, and the measurements with an R^2 values of < 0.70 are recommended to be ineligible by the manufacturer. In clinical trials using ATI, the eligibility criteria often included an R^2 value of ≥ 0.80, which is met by most cases [10)-13)]. However, in clinical practice, an R^2 value of < 0.80 is often observed, with no consensus on the factors that affect R^2 value. Therefore, this study aimed to the R^2 value of patients who underwent ATI in clinical practice and investigates the factors influencing R^2 values. Our results will provide deeper insights into the link between R^2 values and liver-associated pathologies.

II. Materials and Methods

Study population

This retrospective cohort study analyzed the data of patients who underwent ATI for the evaluation of hepatic steatosis at our Hospital between June 2021 and November 2021. The inclusion criteria were: 1) ≥ 16 years of age; 2) no acute hepatitis, drug-induced liver injury, infectious diseases, nephrosis, or cancer; 3) no pregnancy; and 4) no anatomically difficult cases for ATI, such as right lobectomy, multiple liver cysts, and pneumobilia.

This study was approved by our university Institutional Review Board (ID: 332-186). Informed consents were obtained using an opt-out option on our website, and the patients who did not provide informed consents were excluded. This study was conducted in accordance with the principles of the Declaration of Helsinki.

Clinical and laboratory data

Baseline parameters of each patient such as age, sex, height, weight, and daily alcohol consumption were recorded on the day of ATI examination. The NAFLD criteria of alcohol consumption were defined as ethanol intake of < 210 and < 140 g per week for males and females, respectively [14)]. In all cases, the serum levels of aspartate aminotransferase (AST), alanine aminotransferase (ALT), and albumin, and the platelet count (PLT) were measured using standard biochemical methods within 1 month of ATI examination at our hospital laboratory. Patients were identified as having diabetes if they were receiving oral hypoglycemic drug or insulin treatment for diabetes, or had hemoglobin A1c (HbA1c) ≥ 6.5% or fasting blood glucose ≥ 126 mg/dL or random blood glucose ≥ 200 mg/dL [15)].

Abdominal ultrasound examination

All abdominal US examinations were conducted by one of the five ultrasonographers (N.O., K.A., Y.T., C.K., and N.S., all with more than seven years of experience) using a US scanner (Aplio i700; Canon Medical System, Otawara, Japan) with a 1-to-8-MHz convex probe (PVI-475BX). All patients were fasted for at least 6 h before the examination, which was performed in the supine position with the right arm extended above the head. In B-mode examination, either the bright liver or hepato-renal echo contrast were used as the diagnostic criteria for fatty liver [16)]. All 2D shear-wave elastography (SWE) examinations were conducted in the right liver lobe through the intercostal space. The SWE measurement methods were as per previous reports [17)].

ATI examination

After B-mode examination, ATI examination was performed in the right liver lobe through the intercostal window. A fan-shaped sample box was placed on the right liver lobe parenchyma, and a 2 × 3 cm measurement ROI (m-ROI) was placed as previously described [18)]. In brief, an m-ROI was placed around the center of the image, avoiding vessels and shadowing. The top edge of the m-ROI was set at twice the depth of the liver capsule to avoid artifacts.

The AC value (dB/cm/MHz) appeared immediately after the placement of m-ROIs at the bottom of the image. In addition, the goodness of fit of the line profile was displayed as an R^2 value next to the AC, which indicated the reliability of the results. The R^2 values were categorized into poor ($R^2 < 0.70$), good ($0.70 \leq R^2 < 0.90$), and excellent ($R^2 \geq 0.90$) by the manufacturer, which were displayed in red, yellow, and white, respectively. The AC measurements with R^2 values of ≥ 0.70 were considered valid in this study, and the median values were calculated from five different measurements. The principle and detailed measurement protocol of ATI were presented in a previous review [9)].

Statistical analysis

Continuous variables are expressed as medians and ranges. Groups were compared using the Chi-square and Kruskal-Wallis tests for the categorical and quantitative data, respectively. The Spearman rank correlation was used to quantify the association among continuous variables. Further, logistic regression analysis was used to

identify significant risk factors for low R^2 values (< 0.80). Based on previous reports [10)-13), 18)-21)], in the statistical analysis of this study, an AC of < 0.60 is diagnosed as the non-fatty liver. All statistical tests were two-sided, and $P < 0.05$ was considered statistically significant. All statistical analyses were performed using JMP Pro 15.2.1 (SAS, Cary, NC, USA).

III. Results

Patient characteristics

A total of 750 patients were initially included in this study; one patient with hepatitis B virus (HBV)-related cirrhosis was excluded due to low R^2 value (< 0.70). **Table 1** lists the baseline clinical characteristics of the study patients. A total of 190 patients (25%) were obese (BMI ≥ 25 kg/m^2). Further, 674 patients (90%) displayed alcohol consumption that met the NAFLD criteria. Diabetes was complicated in 154 (21%) cases.

Ultrasound findings

The median subcutaneous thickness and shear-wave speed were 16.2 mm and 1.30 m/sec, respectively (**Table 2**). The median AC was 0.58 dB/cm/MHz, and the AC value represented a graph that spread to both sides of the scale with the peak at 0.55 to 0.59 dB/cm/MHz (**Figure 1A**). The diagnostic rate of fatty liver was 34% and 41% for B-mode findings (bright liver or/and hepato-renal echo contrast) and ATI (AC ≥ 0.60 dB/cm/MHz), respectively. The median R^2 value was 0.87; R^2 values of ≥ 0.90, 0.80 to 0.89, and 0.70 to 0.79 were observed in 290 (39%), 350 (47%), and 109 (15%) patients, respectively (**Figure 1B**).

Effects of the inter-ultrasonographer comparisons

The measurements of AC and R^2 values were compared

Table 1 Baseline clinical characteristics of the patients (n = 749)

Age, years	67 (16 – 94)
Male	315 (42)
BMI, kg/m^2	22.5 (13.6 – 43.1)
Alcohol intake	
Meet the NAFLD criteria	674 (90)
Diabetes	154 (21)
AST, U/L	22 (4 – 263)
ALT, U/L	19 (2 – 236)
Albumin, g/dL	4.1 (2.4 – 5.2)
Platelet count, × 10^4 μL	20.9 (4.7 – 65.5)
FIB-4 index	1.68 (0.28 – 10.74)

- *Note*: Data are shown as n(%), or median(range).
- Abbreviations: BMI, body mass index; NAFLD, non-alcoholic fatty liver disease; AST, aspartate transaminase; ALT, alanine transaminase.
- FIB-4 index = (AST × Age) / (Platelet count × √ALT)

Table 2 Ultrasound results in this study (n = 749)

Skin-capsule (SC) distance, mm	16.2 (8.5 – 40.4)
Capsule-ROI (CR) distance, mm	18.6 (6.3 – 34.0)
Skin-ROI distance, mm	35.1 (18.1 – 64.2)
Ratio of SC/CR	0.87 (0.31 – 2.40)
Shear-wave speed, m/sec	1.30 (0.91 – 3.21)
B-mode	
Bright liver	244 (33)
Hepato-renal echo contrast	237 (32)
AC, dB/cm/MHz	0.58 (0.33 – 1.17)
Diagnosis of fatty liver	
B-mode	252 (34)
AC ≥ 0.60	307 (41)
AC ≥ 0.66	222 (30)
R^2	0.87 (0.70 – 0.98)

- *Note*: Data are shown as n(%), or median(range). Abbreviations: ROI, region of interest; AC, Attenuation coefficient; R^2, coefficient of determination.

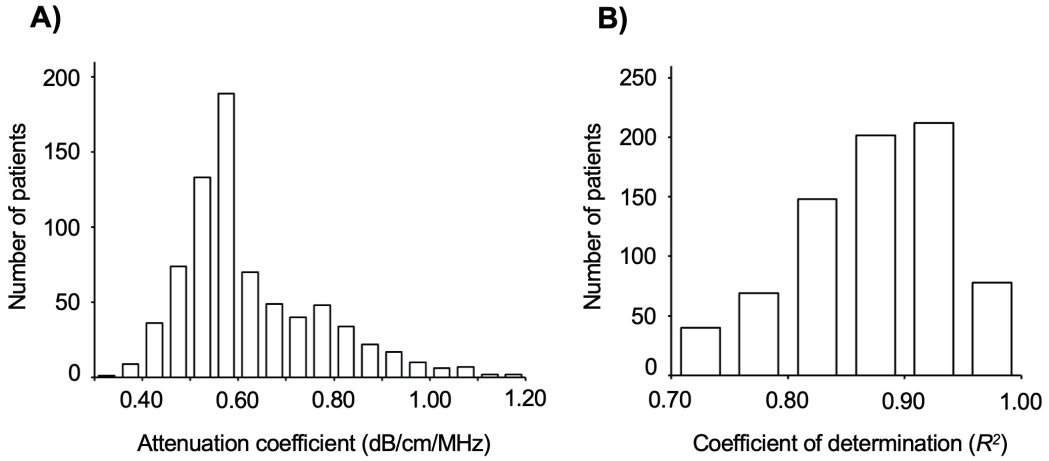

Figure 1 Bar chart for attenuation coefficient (AC) and coefficient of determination (R2) measurement results (n = 749).
(A) The median AC was 0.58 dB/cm/MHz; the AC value spreads to both sides of the axis with the peak at 0.55 to 0.59 dB/cm/MHz.
(B) The median R2 value was 0.87, with 109 cases (15%) having R2 value range of 0.70 to 0.79.

with the ultrasonographers. A significant difference was observed in the prevalence of diabetes ($P = 0.003$) and shear-wave speed ($P < 0.001$) in the baseline characteristics of the patients (**Table 3**). However, no significant differences were observed in the measurements of the AC and R^2 values among ultrasonographers (**Figure 2A, B**).

Correlations between clinical findings and the coefficient of determination (R^2)

AC was identified as the most highly correlated factor (correlation coefficient [r] = 0.842) with R^2 values. Of the 109 cases with R^2 values of < 0.80, 108 patients showed an AC of < 0.60 (**Figure 3**). Furthermore, BMI ($r = 0.521$) and skin-liver capsule distance ($r = 0.525$) also showed relatively strong correlations (**Table 4**).

Determinant factors for t terminatio n (R^2)

Univariate analysis identified the female sex (Odds ratio [OR] 1.64, $P = 0.024$), BMI < 23 kg/m^2 (OR 3.86, $P < 0.001$), uncomplicated diabetes (OR 3.25, $P = 0.001$), ALT < 30 IU/L (OR 2.38, $P = 0.005$), albumin < 4.0 g/dL (OR 1.53, $P = 0.045$), skin-liver capsule distance < 20 mm (OR 6.15, $P < 0.001$), and AC < 0.60 dB/cm/MHz (OR 98.95, $P < 0.001$) as factors significantly associated with low R^2 values (< 0.80) (**Table 5**). However, in multivariate analysis, uncomplicated diabetes (OR 2.68, $P = 0.010$) and AC < 0.60 dB/cm/MHz (OR 72.76, $P < 0.001$) were the only independent determinant factors for low R^2 values.

Discussion

The coefficient of determination (R^2) is an important value as it indicates AC reliability during ATI. However, in clinical practice, the R^2 value and its influencing factors remain uninvestigated. This study showed that the patients with R^2 values of < 0.80 had non-fatty liver, suggesting that the high R^2 values observed in clinical trials were possibly related to the recruitment of a high

Table 3 Patient and ultrasound results by the ultrasonographers (n = 749)

Clinical parameters	Ultrasonographer					P value
	A	B	C	D	E	
Age, years	66	69	67	67	68	0.801
Female	54	60	57	58	63	0.641
BMI, kg/m^2	23.0	22.0	22.9	22.3	21.8	0.188
Diabetes	17	14	31	25	17	0.003
ALT, U/L	20	19	18	18	19	0.651
FIB-4 index	1.73	1.64	1.55	1.75	1.79	0.571
Skin-capsule distance, mm	16.5	15.8	17.1	15.7	15.4	0.166
Shear-wave speed, m/sec	1.29	1.34	1.26	1.30	1.26	<.001
Number of tests	217	153	150	134	95	–

・*Note*: Data are shown as n (%), or median (range).
・Abbreviations: BMI, body mass index; ALT, alanine transaminase; AC, Attenuation coefficient.
・FIB-4 index = (AST × Age) / (Platelet count × $\sqrt{}$ALT)

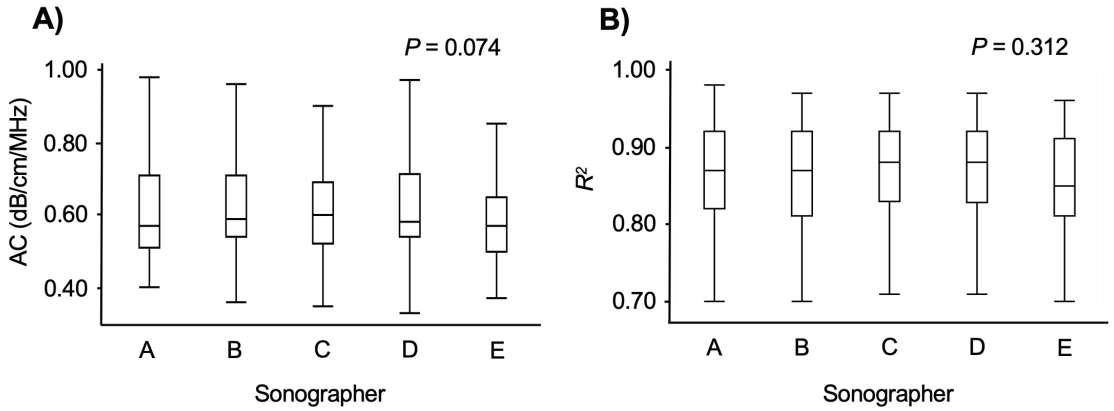

Figure 2 Comparison of attenuation coefficient (AC) and coefficient of determination (R^2) based on the ultrasonographers (n = 749).
(A) AC and **(B)** R^2 values show the comparison based on ultrasonographers; the number of tests conducted was: ultrasonographer A (n = 217); B (n = 153); C (n = 150); D (n = 134); E (n = 95). The results are shown as box plot profiles, with the bottom and top edges of the boxes representing the 25th and 75th percentiles, respectively. Median values are shown by the line within the box.

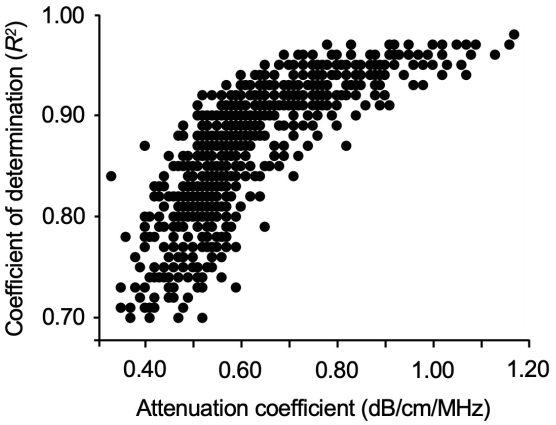

Figure 3 Scatter plots for attenuation coefficient (AC) and coefficient of determination (R^2) (n = 749). The AC and R^2 were strongly correlated (correlation coefficient = 0.842), and of the 109 cases with $R^2 < 0.80$, 108 cases had AC of < 0.60.

Table 4 Correlations between clinical findings and coefficient of determination (R^2) (n = 749)

Clinical parameters	Statistics	
	r	P value
Age, years	− 0.053	0.149
BMI, kg/m^2	0.521	<.001
Skin-capsule distance, mm	0.525	<.001
Capsule-ROI distance, mm	0.183	<.001
ALT, U/L	0.345	<.001
Albumin, g/dL	0.086	0.019
Platelet count, × 10^4 μL	0.092	0.012
FIB-4 index	− 0.085	0.021
Shear-wave speed, m/sec	0.162	<.001
AC, dB/cm/MHz	0.842	<.001

・ Abbreviations: r, correlation coefficient; BMI, body mass index; ROI, region of interest; ALT, alanine transaminase; AC, Attenuation coefficient.
・ FIB-4 index = (AST × Age) / (Platelet count × $\sqrt{}$ALT)

number of patients with fatty liver disease [10)-13)]. Since lower R^2 values were associated with presence of more vessels in the m-ROI, higher R^2 values of fatty livers may indicate obscurement of the vessels. In this study, we also showed a strong correlation of the R^2 value with AC (**Table 4**). Further, uncomplicated diabetes and AC (< 0.60 dB/cm/MHz) were identified as factors that affect R^2 values (**Table 5**).

The mechanism underlying high R^2 values in diabetic patients remains unknown. Previous studies have shown a link between diabetes and CAP; a large cohort study revealed that in addition to information on the hepatic steatosis, CAP could reflect the severity of the metabolic syndrome [6)]. Additionally, in a separate study that utilized linear mixed model meta-analysis data, diabetes was shown to be related to CAP value independent of liver steatosis [7)]. Although the underlying mechanism of the relationship between CAP and diabetes have not been elucidated, epidemiological evidence exists [6)7)]. Further studies are warranted to better understand the mechanism by which diabetes affects the US beam attenuation and R^2 values.

This study showed a difference between the examiners in SWE (**Table 3**). However, no inter-observer differences were observed for AC and R^2 value measurements (**Figure 2A, B**). These results were consistent with those of previous study, wherein good (intraclass correlation coefficient [ICC] 0.792) [22)] or excellent (ICC 0.92) [19)] inter-observer reproducibility has been reported. Although this study is not an analysis of the same subjects, but only a comparison of median values in a large number of cases, we believe that inter-observer variability (for measuring AC and R^2 values) can be eliminated if the measurement methods are standardized within the facility.

Until recently, liver biopsy was the reference standard for the fatty liver diagnosis and remains the only method for confirming a diagnosis of NASH [3)]. However, liver biopsy has several important limitations, including complications such as bleeding, small sample volume, sampling error, and variability of assessment among different pathologists [23)]. These limitations restrict the repetition of liver biopsies to observe histologic changes; therefore, a more accurate non-invasive technique is desired for grading steatosis.

MRI-estimated proton density fat fraction (PDFF) is a quantitative imaging technique that enables accurate, repeatable, and reproducible quantitative assessment of liver steatosis of the whole liver [24)]. The assessment of liver fat using MRI-PDFF has the highest diagnostic accuracy in comparison with any other non-invasive assessment method [5)]. Therefore, MRI-PDFF is the accepted reference standard for the evaluation of liver steatosis [24)]. Despite its strengths, MRI-PDFF is impractical due to associated high costs and unavailability.

In contrast, US-based techniques are advantageous due to their low cost of operation and easy and wide availability. In this context, ATI seems an attractive tool. Kuroda et al. reported that the areas under the receiver operating characteristic (AUROC) curve of ATI for identifying steatosis grade ≥ S1, ≥ S2, and S3 were 0.876, 0.883, and 0.908, respectively, which were significantly better than the results obtained with CAP for identifying S3 (AUROC 0.842, $P = 0.028$) [20)]. In addition, the success rates of ATI and CAP were 100% (111/111) and 94.6% (105/111),

Table 5 Multivariate analysis of factors associated with low value of coefficient of determination ($R^2 < 0.80$)

	No. of patients with low R^2	Crude OR	95% CI	*P* value	Adjusted OR	95% CI	*P* value
Age							
(< 65 years old)	41/315	0.81	0.53 − 1.22	0.310			
(≥ 65 years old)	68/434	1.00 (ref.)					
Sex							
Female	74/434	1.64	1.07 − 2.53	0.024	1.32	0.83 − 2.12	0.242
Male	35/315	1.00 (ref.)			1.00 (ref.)		
BMI							
(< 23.0 kg/m^2)	86/401	3.86	2.37 − 6.27	<.001	1.44	0.83 − 2.49	0.196
(≥ 23.0 kg/m^2)	23/348	1.00 (ref.)			1.00 (ref.)		
Alcohol intake (NAFLD criteria)							
Meet the criteria	101/674	1.48	0.69 − 3.17	0.317			
Not meet the criteria	8/75	1.00 (ref.)					
Diabetes							
No (%)	100/595	3.25	1.61 − 6.60	0.001	2.68	1.26 − 5.70	0.010
Yes (%)	9/154	1.00 (ref.)			1.00 (ref.)		
ALT							
(< 30 U/L)	96/580	2.38	1.30 − 4.37	0.005	0.78	0.39 − 1.57	0.493
(≥ 30 U/L)	13/169	1.00 (ref.)			1.00 (ref.)		
Albumin							
(< 4.0 g/dL)	46/253	1.53	1.01 − 2.31	0.045	1.47	0.94 − 2.31	0.093
(≥ 4.0 g/dL)	63/496	1.00 (ref.)			1.00 (ref.)		
Platelet count							
(< 20.0 × 10^4 μL)	47/322	1.01	0.67 − 1.52	0.977			
(≥ 20.0 × 10^4 μL)	62/427	1.00 (ref.)					
FIB-4 index							
(< 1.30)	35/245	0.97	0.63 − 1.50	0.885			
(≥ 1.30)	74/504	1.00 (ref.)					
Skin-capsule distance							
(< 20 mm)	104/598	6.15	2.46 − 15.4	<.001	1.97	0.72 − 5.39	0.189
(≥ 20 mm)	5/151	1.00 (ref.)			1.00 (ref.)		
Shear-wave speed							
(< 1.30 m/sec)	57/365	1.15	0.76 − 1.73	0.502			
(≥ 1.30 m/sec)	51/368	1.00 (ref.)					
AC							
(<0.60 dB/cm/MHz)	108/442	98.9	13.7 − 713	<.001	72.8	9.87 − 536	<.001
(≥ 0.60 dB/cm/MHz)	1/307	1.00 (ref.)			1.00 (ref.)		

- Abbreviations: OR, odds ratio; CI, confidence interval; BMI, body mass index; NAFLD, non-alcoholic fatty liver disease; ALT, alanine transaminase; AC, Attenuation coefficient; ref., reference.
- FIB-4 index = (AST × Age) / (Platelet count × $\sqrt{}$ALT)

respectively[20].

Data from previous clinical trials using ATI indicate that the most important obstacle for ATI is the non-standardized measurement method. The size and location of the m-ROI as well as the valid cut-off R^2 values varied in previous studies[9]. In the present study, the top edge of the m-ROI was set at twice the depth of the liver capsule. The usefulness of this m-ROI position has recently been reported[21] but was not universally applicable. Even in this study, the ratio of the distance from the skin to the liver capsule and from the liver capsule to the upper end of the m-ROI was 0.87, slightly longer for the capsule–m-ROI (**Table 2**). This is probably due to multiple reflections in some patients with short subcutaneous thickness, leading to setting of the m-ROI deeper than twice.

Being a single-center study was the main limitation of this study as the results could not be generalized. Hence, to validate the results of this pilot study, prospective multicenter studies with a large number of patients are required. All the study participants were Japanese, and since ethnicities correlate with several disease conditions, further studies with patients of various ethnic groups are required to validate the results of this study in other ethnic populations.

In conclusion, this study showed that the R^2 values, which represent AC reliability during diagnostic ATI for hepatic steatosis, of < 0.80 were associated with non-fatty liver. Further, AC and diabetes were identified

as independent factors associated with low R^2 values. ATI represents a technique with the scope of widespread diagnostic applications. However, the ATI method should be standardized, and further studies are needed to better understand the mechanism underlying the effects of diabetes on R^2 values.

IV. Authorship Contributions

All authors made substantial contributions to the conception and design of the study. N.O., K.A., Y.T., C.K., and N.S. acquired the data. S.Tanaka analyzed and interpreted the data. S.Tanaka was the chief investigator and was responsible for the data analysis. N.O., K.A., K.Y. and K.M. provided logistical support and discussed the data. S.Takahashi and J.K. directed the overall project. All authors contributed to the writing of the final manuscript and provided final approval of the submitted version.

Acknowledgement

The authors would like to thank Editage (www.editage.com) for English language editing.

Conflict of interest statements

The authors declare that they have no conflict of interest associated with this study.

Funding sources

None.

References

1) Huang DQ, El-Serag HB, Loomba R. Global epidemiology of NAFLD-related HCC: Trends, predictions, risk factors and prevention. Nat Rev Gastroenterol Hepatol 2021; 18(4): 223-38. doi: 10.1038/s41575-020-00381-6.
2) McPherson S, Hardy T, Henderson E, et al. Evidence of NAFLD progression from steatosis to fibrosing-steatohepatitis using paired biopsies: Implications for prognosis and clinical management. J Hepatol 2015; 62(5): 1148-55. doi: 10.1016/j.jhep.2014.11.034.
3) Tokushige K, Ikejima K, Ono M, et al. Evidence-based clinical practice guidelines for nonalcoholic fatty liver disease/nonalcoholic steatohepatitis 2020. Hepatol Res 2021; 51(10): 1013-25. doi: 10.1111/hepr.13688.
4) Hernaez R, Lazo M, Bonekamp S, et al. Diagnostic accuracy and reliability of ultrasonography for the detection of fatty liver: A meta-analysis. Hepatology 2011; 54(3): 1082-90. doi: 10.1002/hep.24452.
5) Tamaki N, Ajmera V, Loomba R. Non-invasive methods for imaging hepatic steatosis and their clinical importance in NAFLD. Nat Rev Endocrinol 2022; 18(1): 55-66. doi: 10.1038/s41574-021-00584-0.
6) Lédinghen V de , Vergniol J, Capdepont M, et al. Controlled attenuation parameter (CAP) for the diagnosis of steatosis: A prospective study of 5323 examinations. J Hepatol 2014; 60(5): 1026-31. doi: 10.1016/j.jhep.2013.12.018.
7) Karlas T, Petroff D, Sasso M, et al. Individual patient data meta-analysis of controlled attenuation parameter (CAP) technology for assessing steatosis. J Hepatol 2017; 66(5): 1022-30. doi: 10.1016/j.jhep.2016.12.022.
8) Castera L, Friedrich-Rust M, Loomba R. Noninvasive assessment of liver disease in patients with nonalcoholic fatty liver disease. Gastroenterology 2019; 156(5): 1264-81. doi: 10.1053/j.gastro.2018.12.036.
9) Lee DH. Quantitative assessment of fatty liver using ultrasound attenuation imaging. J Med Ultrason (2001) 2021; 48(4): 465-70. doi: 10.1007/s10396-021-01132-z.
10) Bae JS, Lee DH, Lee JY, et al. Assessment of hepatic steatosis by using attenuation imaging: A quantitative, easy-to-perform ultrasound technique. Eur Radiol 2019; 29(12): 6499–507. doi: 10.1007/s00330-019-06272-y.
11) Jeon SK, Lee JM, Joo I, et al. Prospective evaluation of hepatic steatosis using ultrasound attenuation imaging in patients with chronic liver disease with magnetic resonance imaging proton density fat fraction as the reference standard. Ultrasound Med Biol 2019; 45(6): 1407-16. doi: 10.1016/j.ultrasmedbio.2019.02.008.
12) Burgio DM, Ronot M, Reizine E, et al. Quantification of hepatic steatosis with ultrasound: Promising role of attenuation imaging coefficient in a biopsy-proven cohort. Eur Radiol 2020; 30(4): 2293-301. doi: 10.1007/s00330-019-06480-6.
13) Sugimoto K, Moriyasu F, Oshiro H, et al. The role of multiparametric US of the liver for the evaluation of nonalcoholic steatohepatitis. Radiology 2020; 296(3): 532-40. doi: 10.1148/radiol.2020192665.
14) Chalasani N, Younossi Z, Lavine JE, et al. The diagnosis and management of nonalcoholic fatty liver disease: Practice guidance from the American association for the study of liver diseases. Hepatology 2018; 67(1): 328-57.
15) Cosentino F, Grant PJ, Aboyans V, et al. 2019 ESC Guidelines on diabetes, pre-diabetes, and cardiovascular diseases developed in collaboration with the EASD. Eur Heart J 2019; 41(2): 255-323. doi: 10.1093/eurheartj/ehz486.
16) Hamaguchi M, Kojima T, Itoh Y, et al. The severity of ultrasonographic findings in nonalcoholic fatty liver disease reflects the metabolic syndrome and visceral fat accumulation. Am J Gastroenterol 2007; 102(12): 2708–15. doi: 10.1111/j.1572-0241.2007.01526.x.
17) Ferraioli G, Wong VW-S, Castera L, et al. Liver ultrasound elastography: An update to the world federation for

ultrasound in medicine and biology guidelines and recommendations. Ultrasound Med Biol 2018; 44(12): 2419–40. doi: 10.1016/j.ultrasmedbio.2018.07.008.

18) Tada T, Iijima H, Kobayashi N, et al. Usefulness of attenuation imaging with an ultrasound scanner for the evaluation of hepatic steatosis. Ultrasound Med Biol 2019; 45(10): 2679-87. doi: 10.1016/j.ultrasmedbio.2019.05.033.

19) Jesper D, Klett D, Schellhaas B, et al. Ultrasound-based attenuation imaging for the inter-observer variability. IEEE J Transl Eng Health Med 2020; 8: 1-9.

20) Kuroda H, Abe T, Fujiwara Y, et al. Diagnostic accuracy of ultrasound-guided attenuation parameter as a noninvasive test for steatosis in non-alcoholic fatty liver disease. J Med Ultrason(2001) 2021; 48(4): 471-80. doi: 10.1007/s10396-021-01123-0.

21) Sugimoto K, Abe M, Oshiro H, et al. The most appropriate region-of-interest position for attenuation coefficient measurement in the evaluation of liver steatosis. J Med Ultrason(2001) 2021; 48(4): 615–21. doi: 10.1007/s10396-021-01124-z.

22) Yoo J, Lee JM, Joo I, et al. Reproducibility of ultrasound attenuation imaging for noninvasive evaluation of hepatic steatosis. Ultrasonography 2020; 39(2): 121-9.

23) Davison BA, Harrison SA, Cotter G, et al. Suboptimal reliability of liver biopsy evaluation has implications for randomized clinical trials. J Hepatol 2020; 73(6): 1322-32. doi: 10.1016/j.jhep.2020.06.025.

24) Caussy C, Reeder SB, Sirlin CB, et al. Noninvasive, quantitative assessment of liver fat by MRI-PDFF as an endpoint in NASH trials. Hepatology 2018; 68(2): 763-72. doi: 10.1002/hep.29797.

Original

Absolute lymphocyte count is a prognostic predictor in patients with recurrent HER2-negative breast cancer treated with eribulin

Seiichi Mokuyasu[*1], *Risa Oshitanai*[*2], *Toru Morioka*[*2], *Yuki Saito*[*2], †*Yasuhiro Suzuki*[*2]

†Correspondence: Department of Breast Surgery, Tokai University Hachioji Hospital, Tokai University School of Medicine
1838 Ishikawa, Hachioji, Tokyo 192-0032, Japan
E-mail: luke-szk@is.icc.u-tokai.ac.jp
Received February 7, 2023; accepted October 5, 2023
*1 Department of Clinical Laboratory, Tokai University Hachioji Hospital, Tokyo, Japan
*2 Department of Breast Surgery, Tokai University Hachioji Hospital, Tokai University School of Medicine, Tokyo, Japan

ABSTRACT

Background: Absolute lymphocyte count (ALC) and neutrophil lymphocyte rate (NLR) as immune system and inflammatory markers have been suggested as prognostic factors in eribulin treatment. However, the respective cut-off values have not been determined. Hence, we investigated the relationship between overall survival (OS) and baseline ALC (bALC) and baseline NLR (bNLR) in eribulin-treated patients with human epidermal growth factor receptor 2 (HER2)-negative breast cancer (BC) by using 2 types of cut-off values for each.
Methods: Univariate and multivariate analyses were performed to investigate the association of bALC and bNLR with OS among 114 female patients with HER2-negative BC treated with eribulin.
Results: The OS of patients with HER2-negative BC was compared based on bALC (cut-off value: 1,200/μL and 1,500/μL) and bNLR (cut-off values: 2 and 3). A significant difference was observed in median OS between patients with bALC of ≥ 1,200/μL and those with bALC of < 1,200/μL (hazard ratio [HR]: 0.596 [0.395, 0.889], p = 0.014). For bNLR (cut-off value: 2), the median OS was significantly higher in patients with a bNLR of < 2 than in those with a bNLR of ≥ 2 (HR: 0.629 [0.406, 0.974], p = 0.038).
Conclusions: Patients with HER2-negative BC with a bALC of ≥ 1,200/μL showed a longer OS than patients with a bALC of < 1,200/μL, thus suggesting that survival prediction using bALC was effective for eribulin-treated patients with recurrent HER2-negative BC. It should be noted that the optimal cut-off value for ALC may change depending on the target patient group.

〔Lab Med Int 2023; 2(3): 50-59〕

Key Words
absolute lymphocyte count, neutrophil lymphocyte rate, HER2-negative breast cancer, eribulin, overall survival

I. Introduction

Breast cancer (BC) is the most commonly diagnosed cancer and the leading cause of cancer-related deaths in women worldwide. Approximately 2.1 million females were newly diagnosed with BC in 2018 globally, accounting for almost 1 in 4 female cancer cases [1]. Breast cancer-related mortality is increasing annually worldwide [2].

Eribulin mesylate (eribulin) is a non-taxane microtubule dynamic inhibitor [3][4]. In Japan, eribulin is used to treat inoperable or recurrent BC [5]. In a phase 3 study (EMBRACE trial), eribulin-treated patients presented significantly longer overall survival (OS) than the patients administered with their physician's therapy of choice [6].

Absolute lymphocyte count (ALC) and neutrophil lymphocyte rate (NLR) are immune system and inflammatory markers and have been reported as indicators of the effectiveness of eribulin therapy [7][8]. Reportedly, a high ALC and low NLR could predict the survival of eribulin-treated patients with BC [9][10]. However, the respective cut-off values have not been determined. Assessment of

the tumor microenvironment is important for BC therapy, and eribulin has tumor immunotherapeutic effects on the microenvironment.

It has been suggested that eribulin has a vascular remodeling effect on the microenvironment [11], an inhibitory epithelial–mesenchymal conversion effect on cancer cells [12,13], and an immune effect on cancer cells [14,15]. Patients with relapsed BC who have been previously treated need treatment that is highly effective in prolonging their lives. Because eribulin is an expensive drug, selecting patients who are likely to benefit from eribulin using simple indicators such as ALC may contribute to drug burden, quality of service, and better prognosis. Therefore, in order to increase the therapeutic benefits of eribulin, it is important to investigate the relationship between baseline ALC (bALC) and baseline NLR (bNLR) and the OS, and to determine an index that predicts the therapeutic effect of recurrent BC.

In this study, we retrospectively analyzed the association between bALC and bNLR and survival in eribulin-treated patients with recurrent HER2-negative BC. Moreover, the relationships between metastasis and OS on the basis of bALC and bNLR were retrospectively investigated. We examined the optimal cut-off values for the patients included in this study.

II. Materials and methods

Study design

The study design was approved by the Institutional Review Board of Tokai University School of Medicine (approval number 22R025). This study was conducted in accordance with the tenets of the Declaration of Helsinki. Obtaining informed consent was expected to be difficult because the subjects were patients who were examined previously. Therefore, an information disclosure document on "research purpose, method, opportunity to refuse research participation, and contact information" was publicized.

Patients

Women with HER2-negative BC (n = 114; median age 59.0, range 31–84, years) diagnosed with recurrent BC and treated with eribulin at the Department of Breast Surgery at Tokai University Hospital in August 2011–May 2017 were examined in this study.

On day 1 (start of eribulin therapy; i.e., baseline), the standard dose of eribulin according to the package insert (1.4 mg/m^2 body surface area) was administered intravenously over 2–5 min once weekly. This treatment was administered for 2 consecutive weeks, followed by no treatment in week 3 as one cycle, and the treatment was repeated for several cycles (8 cycles on average). The starting dose of eribulin was reduced per the discretion of the physician to avoid toxicity (1.1 mg/m^2).

The bALC and bNLR were measured within 3 days of the initial administration of eribulin. We analyzed the data of only the patients with available data on bALC and bNLR. No other exclusion criteria were set.

ALC and NLR calculation and cut-off values

The bALC and bNLR were measured using blood samples collected within 3 days before the initial administration of eribulin. The NLR was calculated by dividing the absolute count of neutrophils by the ALC.

In order to exclude the effects of anti-HER2 therapy, we used 2 types of cut-off values for bALC and bNLR to study whether these biomarkers are associated with OS in eribulin-treated patients with recurrent HER2-negative BC.

A previous studies selected the cut-off values for bALC and bNLR based on values used in other studies or those obtained from receiver operating characteristic curve analyses or the median of the patients [16]. Therefore, the cut-off values selected for ALC were 1,200/μL, which was the median value for the patients in this study, and 1,500/μL, which was the cut-off value used in previous studies [9,17]. The NLR cut-off values were 2, which was the median of the patients in this study, and 3, which was the cut-off in previous studies [10,17].

Statistical analyses

All analyses were performed using the data of patients with available and evaluable bALC and bNLR data.

In this study, we divided the patients based on bALC cut-off values of $< 1{,}200/\mu L$, $\geq 1{,}200/\mu L$, $< 1{,}500/\mu L$, and $\geq 1{,}500/\mu L$, and bNLR cut-off values of < 2, ≥ 2, < 3, and ≥ 3.

OS was defined as the time from the first dose of eribulin to death, or to the last date when the patient was confirmed to be living (censored).

To investigate the latent factors that affect OS, univariate and multivariate Cox regression analyses were performed. The univariate model was used to analyze the hazard ratio (HR) and 95% confidence interval (CI) of various factors. Furthermore, a multivariate Cox regression analysis was performed to evaluate the factors that influence OS.

In order to perform an OS analyses on the basis of bALC or bNLR, Kaplan–Meier curves were drawn to analyze the survival rate of various groups. The median OS (95% CI) was estimated. The Cox proportional hazard model was used to estimate the HR and 95% CI of ALC $< 1{,}200/\mu L$ vs. $\geq 1{,}200/\mu L$ and $< 1{,}500/\mu L$ vs. $\geq 1{,}500/\mu L$. The

HR and 95% CI for NLR ≥ 2 vs. < 2 and ≥ 3 vs. < 3 were similarly estimated.

Kolmogorov–Smirnov test was used to assess the normality of distribution of continuous variables. Two-tailed $p < 0.05$ were considered as statistically significant. The sample size of 114 was based on 80% power and a 0.05 significance level. Statistical analyses were conducted using SPSS software version 26.0 (IBM Corp., Armonk, NY, USA).

III. Results

Patient characteristics

With January 31, 2021 as the last observation point, the mean observation period ± standard deviation (SD) was 630.5 ± 588.7 (11–2282) days, and the median OS was 457.5 days. The data of the 114 eribulin-treated patients with HER2-negative BC with available bALC and bNLR data were analyzed. The bALC values were as follows: 55 patients, < 1,200/μL; 59 patients, ≥ 1,200/μL; 79 patients, < 1,500/μL; and 35 patients, ≥ 1,500/μL. The bNLR values were as follows: 42 patients, < 2, 72 patients, ≥ 2, 74 patients,

Table 1 Patient characteristics by baseline ALC and NLR in patients with HER2-negative breast cancer.

Characteristics, n (%)	ALC < 1,200/μL (n = 55)	ALC ≥ 1,200/ μ L (n = 59)	ALC < 1,500/μL (n = 79)	ALC ≥ 1,500/μL (n = 35)	NLR < 2 (n = 42)	NLR ≥ 2 (n = 72)	NLR < 3 (n = 74)	NLR ≥ 3 (n = 40)
Age								
< 65 years	37 (67.3)	41 (69.5)	55 (69.6)	23 (65.7)	27 (64.3)	51 (70.8)	53 (71.6)	25 (62.5)
≥ 65 years	18 (32.7)	18 (30.5)	24 (30.4)	12 (34.3)	15 (35.7)	21 (29.2)	21 (28.4)	15 (37.5)
ER status								
Positive	34 (61.8)	37 (62.7)	49 (62.0)	22 (62.9)	30 (71.4)	41 (56.9)	48 (64.9)	23 (57.5)
Negative	21 (38.2)	22 (37.3)	30 (38.0)	13 (37.1)	12 (28.6)	31 (43.1)	26 (35.1)	17 (42.5)
PgR status								
Positive	29 (52.7)	26 (44.1)	42 (53.2)	13 (37.1)	25 (59.5)	30 (41.7)	38 (51.4)	17 (42.5)
Negative	26 (47.3)	33 (55.9)	37 (46.8)	22 (62.9)	17 (40.5)	42 (58.3)	36 (48.6)	23 (57.5)
Triple-negative								
No	34 (61.8)	40 (67.8)	51 (64.6)	23 (65.7)	31 (73.8)	43 (59.7)	50 (67.6)	24 (60.0)
Yes	21 (38.2)	19 (32.2)	28 (35.4)	12 (34.3)	11 (26.2)	29 (40.3)	24 (32.4)	16 (40.0)
Metastases								
No	0 (0.0)	0 (0.0)	0 (0.0)	0 (0.0)	0 (0.0)	0 (0.0)	0 (0.0)	0 (0.0)
Yes	55 (100.0)	59 (100.0)	79 (100.0)	35 (100.0)	42 (100.0)	72 (100.0)	74 (100.0)	40 (100.0)
Metastatic site								
Regional lymph node	27 (49.1)	31 (52.5)	38 (48.1)	20 (57.1)	19 (45.2)	39 (54.2)	36 (48.6)	22 (55.0)
Distal lymph node	21 (38.2)	24 (40.7)	31 (39.2)	14 (40.0)	14 (33.3)	31 (43.1)	29 (39.2)	16 (40.0)
Lung	33 (60.0)	19 (32.2)	43 (54.4)	9 (25.7)	13 (31.0)	39 (54.2)	33 (44.6)	19 (47.5)
Liver	24 (43.6)	27 (45.8)	34 (43.0)	17 (48.6)	22 (52.4)	29 (40.3)	36 (48.6)	15 (37.5)
Bone	29 (52.7)	35 (59.3)	44 (55.7)	20 (57.1)	26 (61.9)	38 (52.8)	48 (64.9)	16 (40.0)
Brain	6 (10.9)	3 (5.1)	8 (10.1)	1 (2.9)	2 (4.8)	7 (9.7)	6 (8.1)	3 (7.5)
Visceral	43 (78.2)	43 (72.9)	62 (78.5)	24 (68.6)	30 (71.4)	56 (77.8)	57 (77.0)	29 (72.5)
Number of prior chemotherapy regimens								
1	5 (9.1)	9 (15.3)	7 (8.9)	7 (20.0)	5 (11.9)	9 (12.5)	6 (8.1)	8 (20.0)
2	18 (32.7)	21 (35.6)	27 (34.2)	12 (34.3)	13 (31.0)	26 (36.1)	28 (37.8)	11 (27.5)
3	18 (32.7)	15 (25.4)	25 (31.6)	8 (22.9)	12 (28.6)	21 (29.2)	22 (29.7)	11 (27.5)
4	7 (12.7)	6 (10.2)	8 (10.1)	5 (14.3)	6 (14.3)	7 (9.7)	9 (12.2)	4 (10.0)
≥ 5	7 (12.7)	8 (13.6)	12 (15.2)	3 (8.6)	6 (14.3)	9 (12.5)	9 (12.2)	6 (15.0)
Baseline NLR								
< 2	6 (10.9)	36 (61.0)	—	—	—	—	—	—
≥ 2	49 (89.1)	23 (39.0)	—	—	—	—	—	—
Baseline NLR								
< 3	—	—	41 (51.9)	33 (94.3)	—	—	—	—
≥ 3	—	—	38 (48.1)	2 (5.7)	—	—	—	—
Baseline ALC								
< 1,200/μL	—	—	—	—	6 (14.3)	49 (68.1)		
≥ 1,200/μL	—	—	—	—	36 (85.7)	23 (31.9)		
Baseline ALC								
< 1,500/μL	—	—	—	—	—	—	41 (55.4)	38 (95.0)
≥ 1,500/μL	—	—	—	—	—	—	33 (44.6)	2 (5.0)

< 3, and 40 patients, ≥ 3 (**Table 1**).

The duration of eribulin therapy (mean ± SD) in days for patients with a bALC of < 1,200/μL, ≥ 1,200/μL, < 1,500/μL, and ≥ 1,500/μL was 172.4 ± 166.0, 173.6 ± 165.6 (p = 0.106), 170.6 ± 181.8, and 171.7 ± 144.9 days (p = 0.453), respectively. The duration of eribulin therapy in days for patients with a bNLR of < 2, ≥ 2, < 3, and ≥ 3 was 178.4 ± 168.8, 172.4 ± 165.6 (p = 0.158), 184.0 ± 185.2, and 146.7 ± 139.0 (p = 0.219), respectively.

Factors affecting OS in patients with HER2-negative BC on eribulin

Table 2 shows the results of the univariate and multivariate Cox regression analyses of the factors affecting OS. The univariate Cox regression analysis identified progesterone receptor (PgR) status, bone metastasis, bALC (cut-off value: 1,200/μL), and bNLR (cut-off value: 2) (p = 0.005, p = 0.006, p = 0.014, and p = 0.038) as independent factors that affect OS. Furthermore, the multivariate regression analysis identified PgR status (p = 0.001), bone metastasis (p < 0.001), and bALC (cut-off value: 1,200/μL) (p = 0.042) as independent factors that affect OS.

Comparison of OS by bALC and bNLR

Figure 1 displays the Kaplan–Meier survival curves based on the bALC cut-off value of 1,200/μL and bNLR cut-off value of 2 in patients with HER2-negative BC. The median OS (95% CI) was significantly higher in patients with ALC ≥ 1,200/μL than in patients with ALC < 1,200/μL (676.0 [470.1, 881.9] vs. 361.0 [205.2, 516.8] days) (HR: 0.596 [0.395, 0.899], p = 0.014) (**Fig. 1a**). A significant difference was found in the median OS (95% CI) between patients with bNLR ≥ 2 (371.0 [221.5, 520.5] days) and those with NLR < 2 (676.0 [463.8, 888.2] days) (HR: 0.629 [0.406, 0.974], p = 0.038) (**Fig. 1b**).

Figure 2 displays the Kaplan–Meier survival curves based on the bALC cut-off value of 1,500/μL and bNLR cut-off value of 3 in patients with HER2-negative BC. The median OS (95% CI) was not significantly different between pa-

Table 2 Univariate and multivariate Cox regression: factors affecting overall survival in patients with HER2-negative breast cancer

Factor	Category		Univariate Cox regression				Multivariate Cox regression		
			n	HR	95% CI	p	HR	95% CI	p
Age	< 65 years	Ref	78						
	≥ 65 years		36	0.999	(0.643, 1.551)	0.995			
ER status	Negative	Ref	43						
	Positive		71	0.756	(0.497, 1.150)	0.191			
PgR status	Negative	Ref	59						
	Positive		55	0.553	(0.365, 0.839)	0.005	0.479	(0.311, 0.736)	0.001
Triple-negative	No	Ref	74						
	Yes		40	1.458	(0.953, 2.230)	0.082			
Regional lymph node metastasis	No	Ref	56						
	Yes		58	0.841	(0.557, 1.269)	0.409			
Distal lymph node metastasis	No	Ref	69						
	Yes		45	1.208	(0.797, 1.830)	0.373			
Lung metastasis	No	Ref	62						
	Yes		52	1.053	(0.698, 1.587)	0.807			
Liver metastasis	No	Ref	63						
	Yes		51	1.442	(0.953, 2.180)	0.083			
Bone metastasis	No	Ref	50						
	Yes		64	1.818	(1.184, 2.793)	0.006	2.308	(1.471, 3.619)	<0.001
Brain metastasis	No	Ref	105						
	Yes		9	1.334	(0.644, 2.762)	0.438			
Visceral metastasis	No	Ref	28						
	Yes		86	1.288	(0.790, 2.101)	0.310			
Number of prior chemotherapy regimens	≤ 3		86	0.806	(0.500, 1.299)	0.376			
	> 3	Ref	28						
Baseline ALC	< 1,200/μL	Ref	55						
	≥ 1,200/μL		59	0.596	(0.395, 0.899)	0.014	0.567	(0.328, 0.980)	0.042
Baseline ALC	< 1,500/μL	Ref	79						
	≥ 1,500/μL		35	0.776	(0.490, 1.229)	0.280			
Baseline NLR	< 2		42	0.629	(0.406, 0.974)	0.038	0.836	(0.468, 1.494)	0.546
	≥ 2	Ref	72						
Baseline NLR	< 3		74	0.750	(0.491, 1.147)	0.185			
	≥ 3	Ref	40						

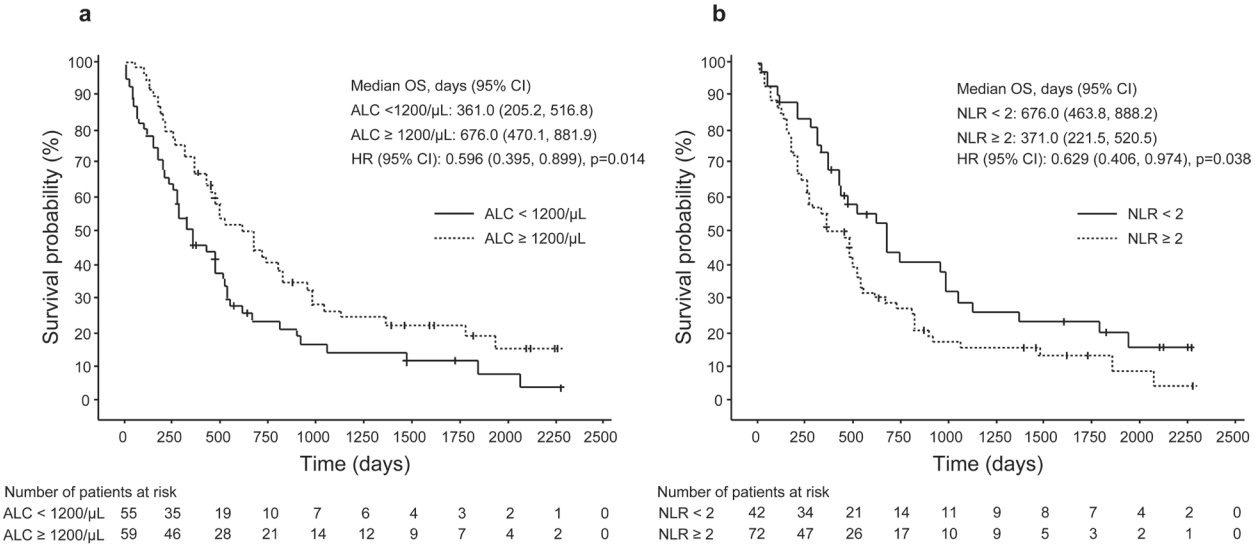

Figure 1

(**a**) shows the Kaplan–Meier survival curve displaying the relationship between bALC (cut-off value: 1,200/μL) and OS in patients with HER2-negative BC. Patients with ALC ≥ 1,200/μL showed a significantly longer OS than patients with ALC < 1,200/μL.

(**b**) shows the Kaplan–Meier survival curve displaying the relationship between bNLR (cut-off value: 2) and OS in patients with HER2-negative BC. Patients with NLR < 2 showed a significantly longer OS than patients with NLR ≥ 2.

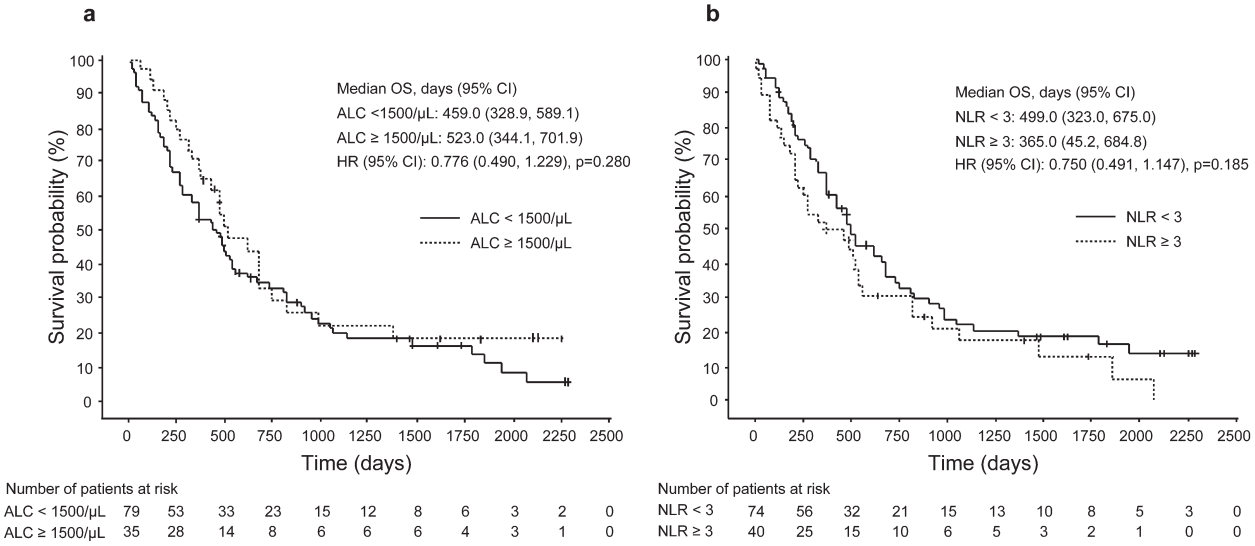

Figure 2

(**a**) shows the Kaplan–Meier survival curve displaying the relationship between bALC (cut-off value: 1,500/μL) and OS in patients with HER2-negative BC. No significant difference was observed between patients with ALC ≥ 1,500/μL and ALC < 1,500/μL.

(**b**) shows the Kaplan–Meier survival curve displaying the relationship between bNLR (cut-off value: 3) and OS in patients with HER2-negative BC. No significant difference was observed between patients with NLR < 3 and patients with NLR ≥ 3.

tients with ALC ≥ 1,500/μL and those with ALC < 1,500/μL (523.0 [344.1, 701.9] vs. 459.0 [328.9, 589.1] days) (HR: 0.776 [0.490, 1.229], p = 0.280) (**Fig. 2a**). A significant difference was not found in the median OS (95% CI) between patients with bNLR ≥ 3 (365.0 [45.2, 684.8]) and those with NLR < 3 (499.0 [323.0, 675.0] days) (HR: 0.750 [0.491, 1.147], p = 0.185) (**Fig. 2b**).

Relationship between metastasis and bALC and bNLR

Table 3 shows the results of the univariate and multivariate Cox regression analyses of the relationship

between OS and bALC and bNLR in patients with less than three metastasized organs. There were no significant differences in the bALC and bNLR between patients with bALC and bNLR values above and those with values below the cut-off values of 1,200/μL and 1,500/μL, and 2 and 3, respectively.

Similarly, **Table 4** shows the results of the univariate and multivariate Cox regression analyses of the relationship between OS and bALC and bNLR in patients with three or more metastasized organs. The univariate Cox regression analysis identified PgR status, triple-negative status, and bALC (cut-off value: 1,200/μL) as factors that affect OS (p = 0.002, p = 0.031, and p = 0.011, respectively). Furthermore, the multivariate Cox regression analysis identified PgR status (p = 0.004) and bALC (cut-off value: 1,200/μL) (p = 0.003) as independent factors that affect the OS.

Relationship between OS by bALC and bNLR and the number of chemotherapy regimens

Table 5 shows the effects of the number of chemotherapy regimens on the bALC and bNLR. When the number of chemotherapy regimens was ≤ 3 or > 3, only bALC (cut-off value: 1,200/μL) showed a significant difference in the median OS (95% CI) (p = 0.037 and p = 0.009). However, the bNLR did not show a significant difference in the median OS (95% CI) (p = 0.053 and p = 0.072).

IV. Discussion

Neutrophils are the primary inflammatory cells involved in tumor cell growth and angiogenesis, modulated by

Table 3 Univariate and multivariate Cox regression: factors affecting overall survival in patients with HER2-negative and < 3 metastatic organ breast cancer

Factor	Category		Univariate Cox regression				Multivariate Cox regression		
			n	HR	95% CI	p	HR	95% CI	p
Age	< 65 years	Ref	19						
	≥ 65 years		15	0.779	(0.344, 1.761)	0.548			
ER status	Negative	Ref	15						
	Positive		19	1.018	(0.453, 2.288)	0.965			
PgR status	Negative	Ref	21						
	Positive		13	0.537	(0.208, 1.387)	0.199			
Triple-negative	No	Ref	20						
	Yes		14	1.202	(0.533, 2.708)	0.657			
Baseline ALC	< 1,200/μL	Ref	16						
	≥ 1,200/μL		18	0.733	(0.326, 1.649)	0.453	0.764	(0.269, 2.173)	0.614
Baseline ALC	< 1,500/μL	Ref	23						
	≥ 1,500/μL		11	0.771	(0.305, 1.948)	0.582	0.930	(0.281, 3.075)	0.905
Baseline NLR	< 2		14	0.631	(0.269, 1.480)	0.290			
	≥ 2	Ref	20						
Baseline NLR	< 3		18	0.611	(0.272, 1.370)	0.232			
	≥ 3	Ref	16						

Table 4 Univariate and multivariate Cox regression: factors affecting overall survival in patients with HER2-negative and ≥ 3 metastatic organ breast cancer

Factor	Category		Univariate Cox regression				Multivariate Cox regression		
			n	HR	95% CI	p	HR	95% CI	p
Age	< 65 years	Ref	59						
	≥ 65 years		21	1.345	(0.789, 2.294)	0.276			
ER status	Negative	Ref	28						
	Positive		52	0.610	(0.371, 1.003)	0.051			
PgR status	Negative	Ref	38						
	Positive		42	0.469	(0.287, 0.765)	0.002	0.350	(0.173, 0.711)	0.004
Triple-negative	No	Ref	54						
	Yes		26	1.752	(1.053, 2.916)	0.031	0.756	(0.367, 1.556)	0.448
Baseline ALC	< 1,200/μL	Ref	39						
	≥ 1,200/μL		41	0.534	(0.329, 0.867)	0.011	0.465	(0.282, 0.769)	0.003
Baseline ALC	< 1,500/μL	Ref	56						
	≥ 1,500/μL		24	0.794	(0.467, 1.350)	0.394			
Baseline NLR	< 2		28	0.651	(0.390, 1.089)	0.102			
	≥ 2	Ref	52						
Baseline NLR	< 3		56	0.703	(0.418, 1.181)	0.183			
	≥ 3	Ref	24						

Table 5 Relationship between overall survival by baseline ALC, NLR, and the number of chemotherapy regimens

Factor	Category		Univariate Cox regression			
			n	HR	95% CI	p
Number of chemotherapy regimens ≤ 3						
Baseline ALC	< 1,200/μL	Ref	41			
	≥ 1,200/μL		45	0.575	(0.341, 0.967)	0.037
Baseline NLR	< 2		30	0.571	(0.323, 1.008)	0.053
	≥ 2	Ref	56			
Number of chemotherapy regimens > 3						
Baseline ALC	< 1,200/μL	Ref	14			
	≥ 1,200/μL		14	0.300	(0.122, 0.738)	0.009
Baseline NLR	< 2		12	0.429	(0.170, 1.077)	0.072
	≥ 2	Ref	16			

the production of cytokines, chemokines and immunosuppression [17]. In addition, lymphocytes also play a role in immunity, and a reduction in their population lowers immune activity against the tumor [18]. For this reason, the NLR, which is a composite indicator of neutrophil and lymphocyte counts, has been suggested to be an effective tumor assessment parameter, as it relates to patient survival [10)17)].

The mechanism of lymphocyte suppression and reduction involves transforming growth factor beta (TGF-β) signaling. TGF-β is an effector of angiogenesis and is produced by tumor cells and prostaglandin E2 (PGE2), which induces suppressor T cells to suppress cancer antigen-specific T cells [19]. Furthermore, the chemokine secretion by tumor cells increases the populations of inflammatory cells such as neutrophils, which are considered to promote tumor cell proliferation via the induction of cytokine secretion from inflammatory cells [20]. Thus, neutrophil count increase and lymphocyte count decrease promote the growth of tumor cells and inhibit the cancer immune response.

In recent studies, it has been shown that inflammatory indicators such as ALC, NLR, platelet-to-lymphocyte ratio (PLR), prognostic nutritional index (PNI), and tumor-infiltrating lymphocytes (TIL) are useful for predicting prognosis in BC. ALC in patients with BC with new metastases tends to decrease, and it has been reported that monitoring the changes in ALC may be useful in assessing the response and prognosis to eribulin treatment [21)22)]. It is also expected that there is a positive correlation between ALC and increased TIL populations [23]. NLR is a predictor of complete pathologic response (pCR) in patients with BC after neoadjuvant therapy [24], and elevated NLR and PLR are suggested to be associated with low OS and high risk of recurrence in patients with BC [25]. In addition, a comparison of PNI and NLR suggested that PNI is an excellent prognostic marker in eribulin-treated patients with metastatic BC [26]. Thus, in recent years, an increasing number of studies have focused on the importance of inflammatory markers as an indicator of systemic tumor immune response. However, previous studies on NLR as a predictor of prognosis in eribulin-treated patients have shown varied results. While many studies have reported an association between bNLR and progression-free survival (PFS) and clinical symptoms [10)27)-29)], other studies have contrarily reported that NLR is not a predictor of OS [9)17)]. One study has reported ALC to be an independent predictor of prolonged OS in eribulin-treated patients with metastatic BC [17].

In this study, we analyzed eribulin-treated patients with recurrent HER2-negative BC to exclude the effects of anti-HER2 therapy from the analysis. The ALC and NLR cut-off values were selected based on receiver operating characteristic curve analyses or cut-off values used in other studies; namely, previously used cut-off values for ALC ranges between 1,000 and 1,500/μL and those for NLR ranges between 2 and 5 [9)17)27)-30)]. To the best of our knowledge, only a limited number of studies have used the median cut-off value that was used in this study. Two cut-off values of bALC and bNLR were used in this study: the median ALC/NLR of the patients in the study (ALC: 1,200/μL, NLR: 2) and the values used in previous studies (ALC: 1,500/μL, NLR: 3). Patients grouped based on the bALC cut-off of 1,200/μL and bNLR of 2 to compare OS resulted in a significant difference in the median OS (95% CI). The multivariate Cox regression analysis results suggested bALC cut-off of 1,200/μL to be independently associated with OS, whereas patients with a bALC of ≥ 1,200/μL showed a significantly longer OS than those with bALC of a < 1,200/μL. As lymphocytes are associated with immunity, this finding implicated that patients with a high bALC have stronger anti-tumor immunity. In contrast, no significant differences were

observed in the OS between patients with bALC ≥ 1,500/μL and those with bALC < 1,500/μL and between patients with NLR ≥ 3 and those with NLR < 3. As such, this study suggested that the median ALC cut-off value of 1,200/μL of the patients in this study was more effective than the cut-offs of ALC 1,500/μL and NLR 3 used in previous studies for predicting the survival of patients with HER2-negative BC. However, the median bALC and bNLR differ in each study. Moreover, the bALC might be affected by individual patient characteristics [27], so it is difficult to set the cut-off value for bALC. Similarly, setting the cut-off value for bNLR is also difficult. Thus, selecting the optimal cut-off value requires further investigation.

In the investigation of the relationship with metastasis, we divided patients with < 3 and ≥ 3 metastasized organs into separate groups, as patients were observed with metastases in multiple organs. The OS in the patients with < 3 metastasized organs was not associated with the bALC and bNLR. However, in patients with ≥ 3 metastasized organs, an association was observed between the OS and bALC (cut-off value: 1,200/μL). A higher number of organs with metastasis is considered to suggest tumor cell proliferation, thus indicating that bALC (cut-off value: 1,200/μL) is associated with survival. The association between OS and bALC was only observed in patients with ≥ 3 metastasized organs, but the reason is unclear. However, it was suggested that bALC may indicate the effectiveness of eribulin therapy in patients with ≥ 3 metastasized organs.

We observed an association between the bALC and OS, but not between the bNLR and OS. However, the NLR has been reported to be a general prognostic factor in patients with BC [17]; therefore, it is possible that not only the lymphocyte count, but also NLR, which is a combined indicator of neutrophil and lymphocyte counts, is effective for predicting survival. This should be elucidated in further studies.

This study was based on a small number of patients, and the effects of treatments other than eribulin were not taken into account; therefore, it is possible that they influence the results of the analyses. Furthermore, it is also possible that the optimal cut-off value selection differs between individual patients. Thus, future studies should be performed using a higher number of patients for further investigation on bALC and bNLR cut-off values and the relationship between bALC/bNLR and OS, rate of change in ALC after initiating eribulin therapy, and its relationship with OS.

In summary, this study showed that patients with recurrent HER2-negative BC with bALC ≥ 1,200/μL had a longer OS than patients with bALC < 1,200/μL, regardless of the number of chemotherapy regimens. Furthermore, bALC ≥ 1,200/μL was associated with a longer OS in patients with 3 or more metastasized organs, suggesting that bALC ≥ 1,200/μL is an effective indicator for predicting the survival of patients with recurrent HER2-negative BC. ALC is a simple indicator of immune response that can be obtained by blood tests, and it has the potential for indicating the efficacy of treatment and predicting survival. However, it should be noted that the optimal cut-off value for ALC may change depending on the target patient group.

Conflicts of interest

The authors declare that they have no conflict of interest.

Funding

This work was not funded.

Acknowledgments

We would like to thank all those who cooperated in this study.

Authorship contributions

Seiichi Mokuyasu: Writing – Original draft; Risa Oshitanai: Investigation; Toru Morioka: Investigation; Yuki Saito: Investigation; Yasuhiro Suzuki: Writing – Review and editing.

References

1) Bray F, Ferlay J, Soerjomataram I, et al. Global cancer statistics 2018: GLOBOCAN estimates of incidence and mortality worldwide for 36 cancers in 185 countries. CA Cancer J Clin 2018 ; 68 (6) : 394-424. doi: 10.3322/caac.21492.

2) Lima SM, Kehm RD, Terry MB. Global breast cancer incidence and mortality trends by region, age-groups, and fertility patterns. EClinicalMedicine 2021; 38: 100985. doi: 10.1016/j.eclinm.

3) Halaven (eribulin mesylate) [prescribing information]. Woodcliff Lake, NJ: Eisai Inc. ; 2017.

4) Halaven 0.44 mg/ml solution for injection [summary of product characteristics]. Hertfordshire, UK: Eisai Europe Limited ; 2019.

5) Halaven [Japanese prescribing information]. Tokyo, Japan: Eisai Co., Ltd ; 2016.

6) Cortes J, O'Shaughnessy J, Loesch D, et al. Eribulin monotherapy versus treatment of physician's choice in patients with metastatic breast cancer (EMBRACE) : a phase 3

open-label randomised study. Lancet 2011 ; 377 (9769) : 914-23. doi: 10.1016/S0140-6736 (11) 60070-6.

7) Yamanaka T, Matsumoto S, Teramukai S, et al. The baseline ratio of neutrophils to lymphocytes is associated with patient prognosis in advanced gastric cancer. Oncology 2007; 73 (3-4) : 215-20. doi: 10.1159/000127412.

8) Sarraf KM, Belcher E, Raevsky E, et al. Neutrophil/lymphocyte ratio and its association with survival after complete resection in non-small cell lung cancer. J Thorac Cardiovasc Surg 2009; 137 (2) : 425-8. doi: 10.1016/j.jtcvs.2008.05.046.

9) Araki K, Ito Y, Fukada I, et al. Predictive impact of absolute lymphocyte counts for progression-free survival in human epidermal growth factor receptor 2-positive advanced breast cancer treated with pertuzumab and trastuzumab plus eribulin or nab-paclitaxel. BMC Cancer 2018; 18 (1) : 982. doi: 10.1186/s12885-018-4888-2.

10) Miyagawa Y, Araki K, Bun A, et al. Significant association between low baseline neutrophil-to-lymphocyte ratio and improved progression-free survival of patients with locally advanced or metastatic breast cancer treated with eribulin but not with Nab-paclitaxel. Clin Breast Cancer 2018; 18 (5) : 400-9. doi: 10.1016/j.clbc.2018.03.002.

11) Ueda S, Saeki T, Takeuchi H, et al. In vivo imaging of eribulin-induced reoxygenation in advanced breast cancer patients: a comparison to bevacizumab. Br J Cancer 2016; 114 (11) : 1212-8. doi: 10.1038/bjc.2016.122.

12) Kashiwagi S, Asano Y, Goto W, et al. Mesenchymal-epithelial transition and tumor vascular remodeling in eribulin chemotherapy for breast cancer. Anticancer Res 2018; 38 (1) : 401-10. doi: 10.21873/anticanres.12236.

13) Kaul R, Risinger AL, Mooberry SL. Eribulin rapidly inhibits TGF-β-induced Snail expression and can induce Slug expression in a Smad4-dependent manner. Br J Cancer 2019; 121 (7) : 611-21. doi: 10.1038/s41416-019-0556-9.

14) Goto W, Kashiwagi S, Asano Y, et al. Eribulin promotes antitumor immune responses in patients with locally advanced or metastatic breast cancer. Anticancer Res 2018; 38 (5) : 2929-38. doi: 10.21873/anticanres.12541.

15) Ito K, Hamamichi S, Abe T, et al. Antitumor effects of eribulin depend on modulation of the tumor microenvironment by vascular remodeling in mouse models. Cancer Sci 2017; 108 (11) : 2273-80. doi: 10.1111/cas.13392.

16) Hong J, Chen X, Gao W, et al. A high absolute lymphocyte count predicts a poor prognosis in HER-2- positive breast cancer patients treated with trastuzumab. Cancer Manag Res 2019; 11: 3371-9. doi: 10.2147/CMAR.S187233.

17) Miyoshi Y, Yoshimura Y, Saito K, et al. High absolute lymphocyte counts are associated with longer overall survival in patients with metastatic breast cancer treated with eribulin-but not with treatment of physician' s choice-in the EMBRACE study. Breast Cancer 2020; 27 (4) : 706-15. doi: 10.1007/s12282-020-01067-2.

18) Terzić J, Grivennikov S, Karin E, et al. Inflammation and colon cancer. Gastroenterology 2010; 138 (6) : 2101-14. doi: 10.1053/j.gastro.2010.01.058.

19) Scarlett UK, Rutkowski MR, Rauwerdink AM, et al. Ovarian cancer progression is controlled by phenotypic changes in dendritic cells. J Exp Med 2012; 209 (3) : 495-506. doi: 10.1084/jem.20111413.

20) Koizumi K, Hojo S, Akashi T, et al. Chemokine receptors in cancer metastasis and cancer cell-derived chemokines in host immune response. Cancer Sci 2007; 98 (11) : 1652-8. doi: 10.1111/j.1349-7006.2007.00606.x.

21) Goto W, Kashiwagi S, Takada K, et al. Utility of follow-up with absolute lymphocyte count in patients undergoing eribulin treatment for early detection of progressive advanced or metastatic breast cancer. Anticancer Res 2022; 42 (2) : 939-46. doi: 10.21873/anticanres.15553.

22) Morisaki T, Kashiwagi S, Asano Y, et al. Prediction of survival after eribulin chemotherapy for breast cancer by absolute lymphocyte counts and progression types. World J Surg Oncol 2021; 19 (1) : 324. doi: 10.1186/s12957-021-02441-w.

23) Altundag K. Is there any association between absolute lymphocyte count and increased tumor-infiltrating lymphocytes in metastatic sites in advanced breast cancer patients who get benefit from eribulin treatment? Breast Cancer Res Treat 2020; 181 (3) : 691. doi: 10.1007/s10549-020-05649-8.

24) Cullinane C, Creavin B, O'Leary DP, et al. Can the neutrophil to lymphocyte ratio predict complete pathologic response to neoadjuvant breast cancer treatment? A systematic review and meta-analysis. Clin Breast Cancer 2020; 20 (6) : e675-e681. doi: 10.1016/j.clbc.2020.05.008.

25) Guo W, Lu X, Liu Q, et al. Prognostic value of neutrophil-to-lymphocyte ratio and platelet-to-lymphocyte ratio for breast cancer patients: An updated meta-analysis of 17079 individuals. Cancer Med 2019; 8 (9) : 4135-48. doi: 10.1002/cam4.2281.

26) Oba T, Maeno K, Ono M, et al. Prognostic nutritional index is superior to neutrophil-to-lymphocyte ratio as a prognostic marker in metastatic breast cancer patients treated with eribulin. Anticancer Res 2021; 41 (1) : 445-52. doi: 10.21873/anticanres.14794.

27) Ueno A, Maeda R, Kin T, et al. Utility of the absolute lymphocyte count and neutrophil/lymphocyte ratio for predicting survival in patients with metastatic breast cancer on eribulin: a real-world observational study. Chemotherapy 2019; 64 (5-6) : 259-69. doi: 10.1159/000507043.

28) Myojin M, Horimoto Y, Ito M, et al. Neutrophil-to-lymphocyte ratio and histological type might predict clinical responses to eriburin-based treatment in patients with met-

astatic breast cancer. Breast Cancer 2020; 27(4): 732-8. doi: 10.1007/s12282-020-01069-0.

29) Li X, Dai D, Chen B, et al. The value of neutrophil-to-lymphocyte ratio for response and prognostic effect of neoadjuvant chemotherapy in solid tumors: A systematic review and meta-analysis. J Cancer 2018; 9(5): 861-71. doi: 10.7150/jca.23367.

30) Watanabe J, Saito M, Horimoto Y, et al. A maintained absolute lymphocyte count predicts the overall survival benefit from eribulin therapy, including eribulin re-administration, in HER2-negative advanced breast cancer patients: a single-institutional experience. Breast Cancer Res Treat 2020; 181(1): 211-20. doi: 10.1007/s10549-020-05626-1.

Original

Comparison of target antigen and immunoglobulin isotypes in anti-SARS-CoV-2 antibodies from natural infection and vaccination

Jeong Hui Kim[*1], Ryosuke Kikuchi*[*2†], Atsuo Suzuki*[*1], Rika Watarai*[*1],*
Kaori Goto[*1], Yui Okumura*[*1], Tadashi Matsushita*[*3, 4]*

†Correspondence: Division of Clinical Laboratory, Gifu University Hospital, 1-1 Yanagido, Gifu, 501-1194, Japan.
E-mail: ryosuke@gifu-u.ac.jp
Received June 1, 2023; accepted September 7, 2023
*1 Department of Medical Technique, Nagoya University Hospital
*2 Division of Clinical Laboratory, Gifu University Hospital
*3 Department of Transfusion Medicine, Nagoya University Hospital
*4 Department of Clinical Laboratory, Nagoya University Hospital

ABSTRACT

The immune system produces antibodies following SARS-CoV-2 infection and vaccination. However, we lack comprehensive information about the humoral responses after infection and vaccination, which are similar but might differ in type or amount of produced antibodies. Therefore, we compared different types and amounts of antibodies produced by the immune system in response to infection versus those produced by BNT162b2 (Pfizer/BioNTech) vaccines. Our findings indicated that naturally infected individuals had 14-fold higher anti-SARS-CoV-2 spike protein (anti-S) and 41-fold higher anti-SARS-CoV-2 receptor-binding domain of the viral spike protein (anti-RBD) IgM titers than SARS-CoV-2-naïve vaccinees. Remarkably, naturally infected individuals maintained high levels of IgM antibody titers up to six weeks after symptom onset. A significantly rapid increase in anti-S IgG titers in primary infection was observed, eventually reaching a level similar to that in people who had third booster vaccination. This study revealed the characteristics of the target antigen and immunoglobulin isotypes after natural SARS-CoV-2 infection and COVID-19 vaccination.

〔Lab Med Int 2023; 2(3): 60-66〕

Key Words
SARS-CoV-2, antibody test, CLEIA, natural infection, vaccination

I. Introduction

Coronavirus disease 2019 (COVID-19) has rapidly spread across the globe since its first report in China in December 2019. Owing to their clinical significance, many agents have been investigated as COVID-19 vaccines and evaluated for their efficacy and safety in clinical trials. During the last three years, 183 and 199 COVID-19 vaccine candidates have been developed in clinical and pre-clinical trials, respectively[1]. The target proteins of SARS-CoV-2 antibodies can be classified into three types: the nucleocapsid protein (anti-N), the spike protein S1 domain (anti-S), and the receptor-binding domain of SARS-CoV-2 spike protein (anti-RBD). Current COVID-19 vaccines principally target the viral S protein or its receptor-binding domain to primarily elicit a robust neutralizing antibody response[2]. Notably, anti-RBD IgG titers are significantly correlated with the neutralization of authentic SARS-CoV-2[3)-6)]. The IgM antibody increases temporarily during the early stages of infection, after which the IgG antibody is produced through a class-switch; this antibody is maintained over a prolonged

time[7) 8)]. Therefore, testing for SARS-CoV-2 antibodies could be a valuable approach to assessing the immune response to SARS-CoV-2 infection and the immune response to the vaccination itself.

Immunochromatography and automated immunoassays, such as chemiluminescence immunoassay, electrochemiluminescence immunoassay, and chemiluminescence enzyme immunoassay (CLEIA) are the common SARS-CoV-2 antibody tests routinely used in laboratories. Currently available antibody reagents use the S protein or its receptor-binding domain of SARS-CoV-2 as target antigens, the difference in reactivity against the S or RBD has not been fully revealed. Although several SARS-CoV-2 antibody test kits have been developed as research reagents, they provide insufficient information about their sensitivity and specificity. Furthermore, we have limited information about serum anti-SARS-CoV-2 IgM/IgG levels after both SARS-CoV-2 natural infection and vaccination. The persistence of the effect in preventing infection or the severity of symptoms remains unclarified.

We aimed to clarify the relationship between target antigen and immunoglobulin isotypes by exploring different types and amounts of antibodies conferred by natural infection versus that from the BNT162b2 using six different antibody reagents.

II. Methods

1. Study design and participants

Naturally infected individuals

This retrospective cohort study was performed among patients with COVID-19 who were admitted to Nagoya University Hospital (Japan) from April 2020 to September 2020. The study protocol was approved by the Ethics Committee of Nagoya University Hospital (approval number:2020-0095), and we applied an opt-out method to obtain informed consent for participation in this study by using the poster available for every patient in our hospital. All methods were conducted in compliance with the principles of the 1964 Declaration of Helsinki and its later amendments. All 13 unvaccinated hospitalized patients (49 to 81 years old) with primary infections were included in this study. Serum samples were collected from all patients between 0–9 days after symptom onset. The remaining serum samples were collected after routine testing. A total of 197 sequential serum samples collected up to 47 days after symptom onset were analyzed.

2. SARS-CoV-2-naïve individuals

This retrospective cohort study was performed among healthcare workers at Nagoya University Hospital (Japan) from March 2021 to April 2022. The study protocol was approved by the Ethics Committee of Nagoya University Hospital (approval number:2021-0040), and all participants provided written informed consent. All methods were conducted in compliance with the principles of the Declaration of Helsinki and relevant guidelines. All workers who received mRNA BNT162b2 vaccines were invited to participate voluntarily, and 25 SARS-CoV-2-naïve individuals who were going to receive a three-dose regimen of the BNT162b2 vaccine were finally enrolled. Blood was collected at seven time points: day 0 (before the first dose); day 7(seven days after the first dose); day 21(before or up to three days after the second dose); day 91(two months after the second dose); day 183(five months after the second dose); day 274 (before or up to 14 days after the third dose), and day 365. Serum samples were used for antibody testing.

3. Antibody measurements

Anti-SARS-CoV-2 antibody detection was performed using six HISCL™ SARS-CoV-2 antibody reagents (Sysmex, Kobe, Japan) on the HISCL™-5000 platform[9)]. In this study, the levels of anti-SARS-CoV-2 IgM and IgG antibodies against the nucleocapsid protein (anti-N), spike protein S1 domain (anti-S), and receptor-binding domain (RBD) of SARS-CoV-2 spike protein (anti-RBD) were quantitatively detected. Recombinant S1 and RBD proteins were produced based on the same accession number sequence (YP_009724390). The S1 domain and RBD contained amino acids 12–684 and 319–537, respectively. Recombinant antigens were purified and coupled with magnetic beads as previously described[9]. In the HISCL™ system, the serum sample was first reacted with magnetic beads coupled with SARS-CoV-2– specific recombinant antigens bound to the magnetic beads. After bound/free separation, the antigen-antibody complex was incubated with an alkaline phosphatase-conjugated antibody against human IgG or IgM to form a sandwich immunocomplex. Anti-IgM and -IgG levels were considered reactive or non-reactive, respectively, using cut-off values of 20 and 10 U/mL, respectively.

4. Serum collection

Blood was collected in no additive tubes (plain tubes) and centrifuged at 1,800 g for 10 min. The samples were stored at − 80℃ until further antibody analysis.

5. Statistical analysis

All analyses were performed using R statistical software (version 4.2.1; R Foundation for Statistical Computing) and GraphPad Prism software (version 9.3.1, San Diego, CA, USA). Correlation analysis was performed using Spearman's correlation test. Comparisons be-

tween naturally infected and BNT162b2-vaccinated individuals were analyzed using the non-parametric Mann–Whitney U test. For all analyses, statistical significance was indicated as follows: ns (non-significant; $p > 0.05$), $^{*}(p < 0.05)$, $^{**}(p < 0.005)$, $^{***}(p < 0.0005)$, $^{****}(p < 0.0001)$.

III. Results

1. Demographic and baseline characteristics of naturally infected individuals

Thirteen hospitalized patients with COVID-19 with primary infections among unvaccinated individuals were included in the study. The demographic and clinical characteristics are provided in Table 1. The patients had a median age of 73 years (49–81 years), 15.4% were women, and among these, 53.7% were smokers. Fever was the most common symptom (84.6 %) on admission. Cardiovascular disease was the most common comorbidity (46.2 %), followed by hypertension and type 2 diabetes (38.5%). Four patients (30.8%) underwent hemodialysis.

2. Demographic and baseline characteristics of SARS-CoV-2-naïve individuals

Twenty-five SARS-CoV-2-naïve individuals who received a three-dose regimen of the BNT162b2 vaccine were enrolled in this study. The patient characteristics are presented in Table 2. The mean age of the participants was 39 years (23–63 years), and 76.0% were women. The most prevalent self-reported symptoms at the first dose were pain at the injection site (76.0%), myalgia (32.0%), fatigue (12.0%), and pyrexia (8.0%). The most prevalent self-reported symptoms at the second dose were pain at the injection site (60.0%), fatigue (56.0%), myalgia (44.0%), and pyrexia (36.0%). At the third dose, pain at the injection site (64.0%), fatigue (56.0%), pyrexia (52.0%), and chills (36.0%) were observed. The percentage of participants reporting pain at the injection site was stable between the three doses; the occurrence of pyrexia increased from 8.0% (2/25) at the first dose to 52.0% (13/25) at the third dose.

3. SARS-CoV-2 antibody reactivity patterns

We first analyzed the antibody levels produced from the natural infection and that from the BNT162b2 mRNA vaccination. The natural infection resulted in higher anti-nucleocapsid (N) IgM and IgG levels (**Figure 1**). The median IgG after seven days of symptom onset was 10.6 U/mL (min-max, 0.7–119.5), positive for anti-IgG. In the nucleocapsid, the seroconversion of anti-IgM and IgG occurred simultaneously or sequentially. The BNT162b2 vaccine only encodes the SARS-CoV-2 spike protein, and no anti-N was observed in the vaccinees. Of note, naturally infected individuals maintained high levels of IgM antibody titers up to six weeks after symptom onset. Compared with naturally infected individuals, SARS-CoV-2-naïve vaccines produced a small amount of anti-S and anti-RBD IgM. In the BNT162b2 vaccinees, anti-S IgM and RBD IgM responded only to the first dose and did not respond after the second or third dose.

4. Peak antibody titers

Given that the differences in antibody titers between natural infection and vaccination, we decided to focus on the peak antibody titers in these two groups. In SARS-CoV-2-naïve individuals who had a three-dose regimen of the BNT162b2 vaccine, three peaks were observed; day 21 (before or up to three days after the second dose); day 91 (approximately two months after the second dose); day 274 (before or up to 14 days after the third dose). Anti-S IgM levels peaked three weeks after the first dose, and anti-IgG levels peaked after booster vaccination. (**Figure 1**) Anti-S IgM and anti-RBD IgM were 14- and 41-fold higher in the naturally infected group than in the vaccinated group, respectively (**Figure 2**). In the primary infection, a significant rapid increase in IgG titers with anti-S and anti-RBD was noted, similar to that of the second and third booster shots. The anti-RBD IgG titer in participants with three doses of the BNT162b2 vaccine was higher than that in naturally infected patients at a time point after the third vaccine dose was administered ($p > 0.0001$).

5. Anti-S/RBD ratio

Anti-RBD IgG levels are significantly correlated with the neutralization of authentic SARS-CoV-2[3)-6)]. Therefore, we validated the anti-S/RBD ratio at each time point and compared anti-S and anti-RBD between naturally acquired and vaccine-induced immunity. The BNT162b2 vaccine exhibited convergence of the S/RBD IgG ratio with booster vaccination (**Figure 3**). The S/RBD IgG ratio at 12 months after the first dose was 1.158 (min-max, 0.986–1.490) and the S/RBD IgM ratio was 0.574 (min–max, 0.203–1.151) (**Figure 3**), suggesting that anti-S IgG reflects anti-RBD IgG changes. In contrast, the natural infection did not result in a constant S/RBD antibody ratio compared with vaccination.

6. Discussion

Several studies have reported a relationship between virus neutralization levels and antibody titers measured using serological tests. Anti-RBD IgG titers significantly correlate with the neutralization of SARS-CoV-2[3)-6) 10)-13)]. Therefore, antibody testing can play a critical role in assessing the immune response to SARS-CoV-2 infection

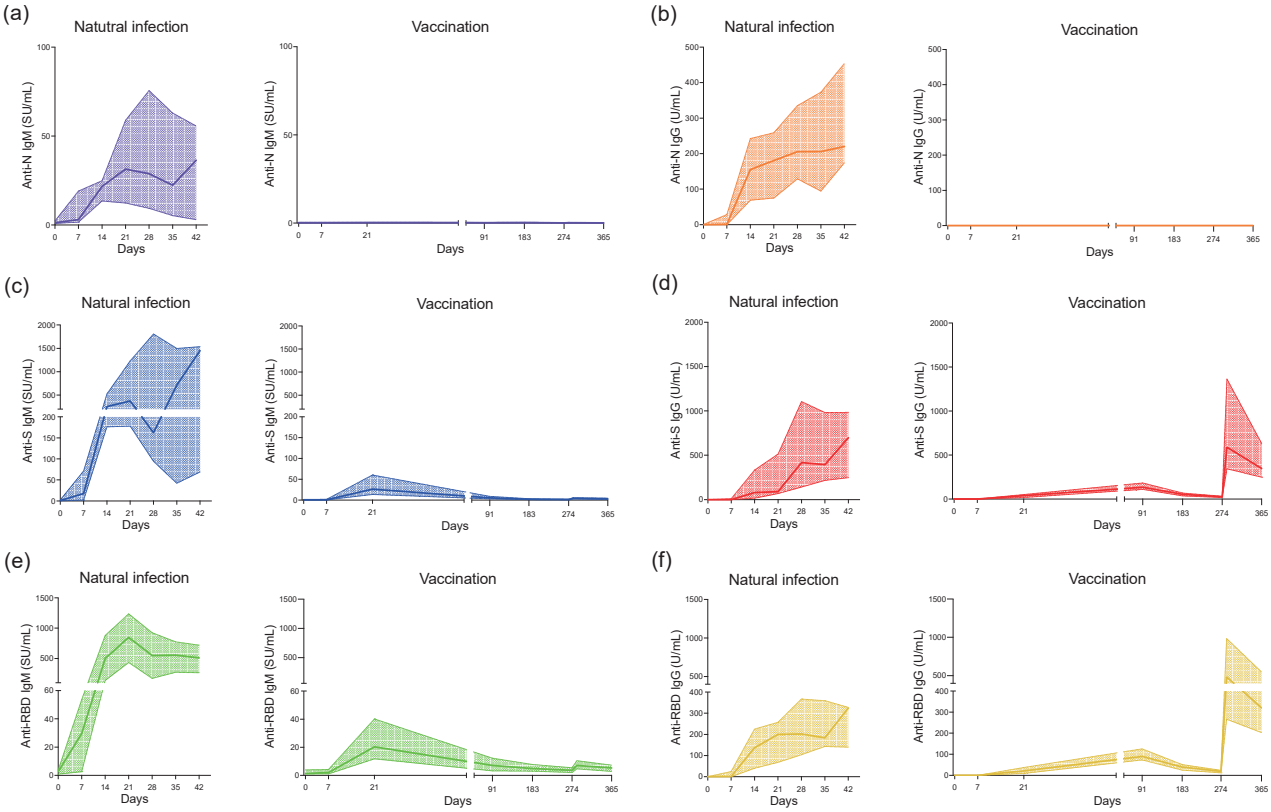

Figure 1 Longitudinal change in antibody titers of natural infection and vaccination.
In natural infection, a total of 197 sequential serum samples from 13 COVID-19 patients collected up to 47 days after symptom onset were analyzed. In vaccination, blood samples were collected from 25 SARS-CoV-2 naïve individuals who received a three-dose regimen of the BNT162b2 vaccine. Blood was collected at seven timepoints up to 365 days after the first-dose.
Anti-IgM titers against the N protein (a), the S protein (c), and the RBD (e); anti-IgG titers against the N protein (b); the S protein (d), and the RBD (f) were determined by performing a CLEIA. Lines of the same color indicate median antibody titers with interquartile range. Manufacturer's positive cut-off concentration sets at 20 SU/mL for IgM, 10 U/mL for IgG.

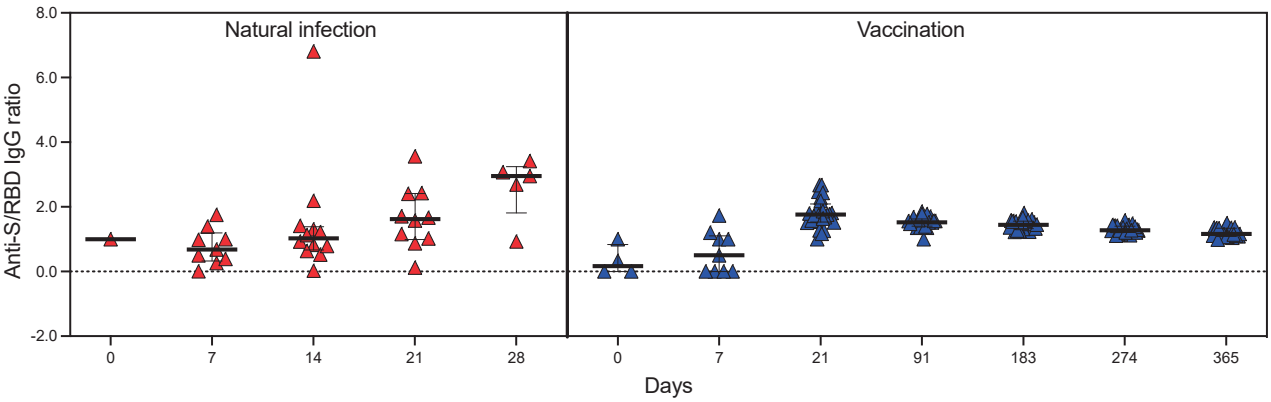

Figure 2 Comparison of anti-S/RBD IgG and IgM ratio in natural infection and vaccination.

and vaccination. To obtain accurate test results, the reactivity of the reagent must be evaluated, and the features and duration of antibody responses to SARS-CoV-2 infection must be defined. Therefore, we evaluated different immunoglobulin isotypes (IgM and IgG) and the levels of antibodies against SARS-CoV-2 N, S, and RBD antigens in longitudinal samples from naturally infected and vaccinated individuals. Our analysis demonstrated that naturally infected individuals maintained high levels of IgM antibody titers up to six weeks after symptom onset, indicating the contribution of antigen-specific memory B cells[16)-18)]. Natural infection could stimulate B cell production via Toll-like receptors (TLRs) to induce downstream signaling, resulting in antibody production and

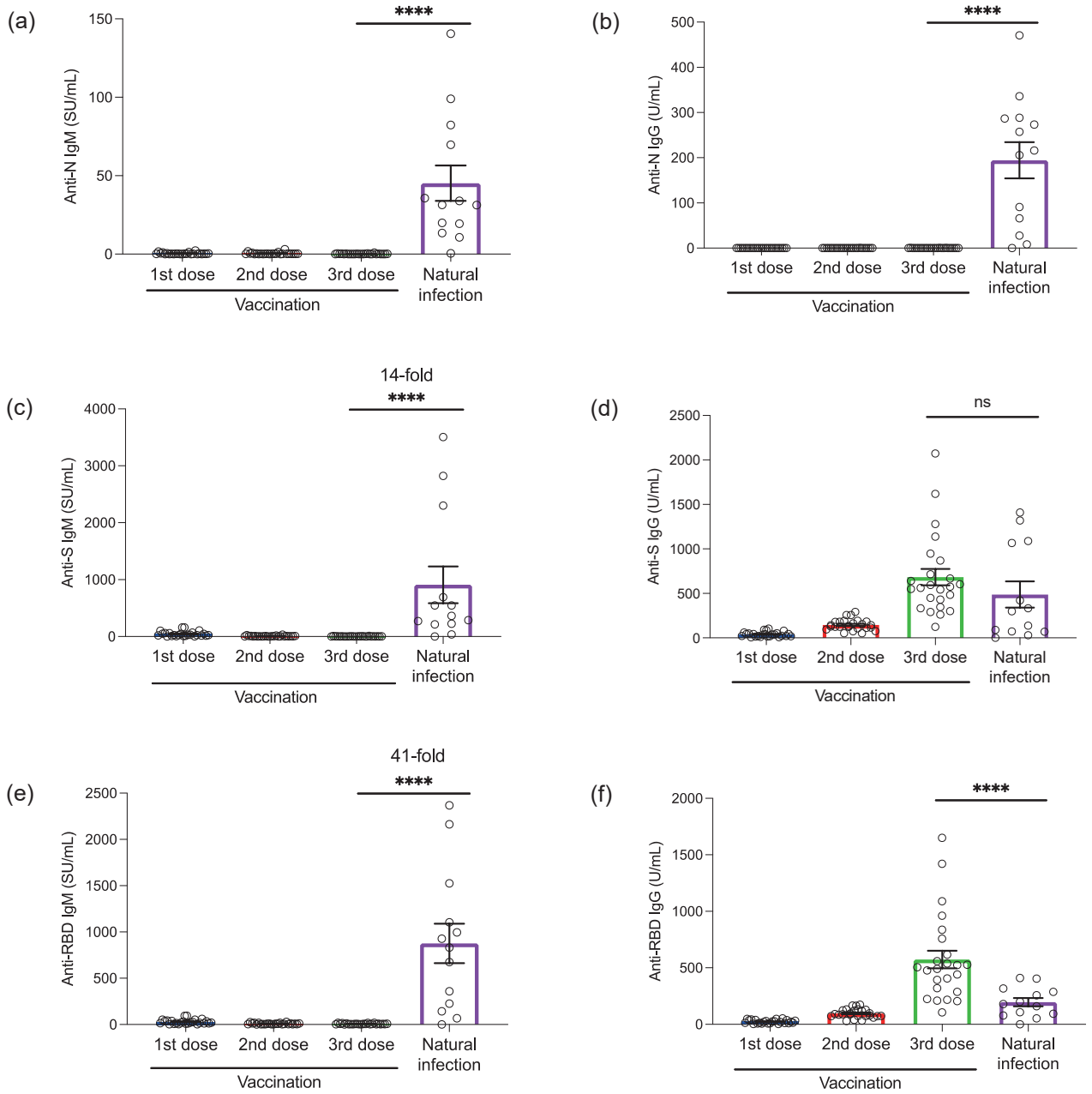

Figure 3 Comparative analysis of peak antibody titers to natural infection and the BNT162b2 mRNA vaccine.
Antibody responses to natural infection and vaccination were assessed by a CLEIA. Anti-IgM peak titers against the N protein (a), the S protein (c), and the RBD (e); anti-IgG peak titers against the N protein (b); the S protein (d), and the RBD (f) were determined. The P value (two-tailed) was calculated using the non-parametric Mann-Whitney U test. ns $p>0.05$, ****$p<0.0001$. Results represent individual values (dots) and means ± the SEM (bars) for anti-IgM and IgG antibodies recognizing N, S, and RBD SARS-CoV-2 antigens.

memory B-cell responses[16)-18)]. According to one study, unlike antibodies, virus-specific memory B cells persist at high levels for at least 12 months post-infection[15]. BNT162b2 mRNA contains N1-methylpseudouridine instead of uridine, which reduces innate immune recognition by TLRs and RIG-I-like receptors [19)]. Vaccination with BNT162b2 mRNA resulted in low IgM antibody titers and low persistence after the first dose, suggesting a primary antibody response by naive B cells[20)]. Taken together, these results suggest that antibody responses during natural infection are maintained by the induction and contribution of IgM memory B cells relative to vaccination.

Naturally infected individuals were diagnosed from April to September 2020, which could be estimated epidemiologically as a mutant strain based on the time of infection[21]. The BNT162b2 mRNA vaccine is a monovalent vaccine containing the original wild-type spike protein of

SARS-CoV-2[19]. As the anti-S and anti-RBD antibodies acquired through infection with mutant strains are derived from antibodies with the mutated S or RBD antigen epitopes, the reactivity of the SARS-CoV-2 antibody reagent may differ from that of wild-type anti-S and anti-RBD antibodies produced by vaccination. Natural infection resulted in higher anti-S and anti-RBD IgG levels, similar to those of participants who had a third booster vaccination; however, caution is warranted in interpreting these data.

In this study, statistical analysis revealed no significant relationship between post-vaccination symptoms and the strength of the antibody responses. However, we observed that most individuals had severe adverse events at the third dose, including pyrexia, and older age was associated with lower titers. We also observed individual differences in the antibody response, and IgM antibody levels helped distinguish people with low and high IgG titers. In the low IgM group, an increase in the IgG titer, comparable to that in the high IgM group, was observed with booster vaccination. This result suggests that higher antibody titers are expected with booster vaccinations, although people have a weakened immune response. Therefore, antibody testing may help generate a vaccination plan for each individual, considering their biochemical background.

Although the S protein or its receptor-binding domain IgG is used to estimate the humoral immune response to the virus, the difference in reactivity against the S or RBD has not been fully revealed. Infectivity-enhancing antibodies recognizing the N-terminal domain (NTD) of the spike are produced following natural infection with SARS-CoV-2. Antibodies to the entire spike protein, including NTD antibodies, may have been produced in the early phase of infection[22)23)]. Thus, the early S/RBD ratio was not as constant as in vaccines. Nevertheless, positive correlation between anti-S IgG and anti-RBD IgG levels was observed not only in the vaccinated group but also in the naturally infected group. Our results are consistent with the results of Wang H et al.[24)], who demonstrated that SARS-CoV-2 RBD-IgG were strongly correlated with S-IgG both in severe and non-severe SARS-CoV-2 patients.

In conclusion, we revealed the characteristics of the target antigen and immunoglobulin isotypes after natural SARS-CoV-2 infection and COVID-19 vaccination.

IV. Limitations of the study

We recognize some limitations in the present study. First, we included only 13 naturally infected and 25 vaccinated individuals; therefore, the sample size was small. In addition, the distribution of age groups in a population and the small sample size of women in the naturally infected group and men in the vaccinated group might have affected the analysis results. Second, information on adverse reactions was obtained using a self-reporting questionnaire. Thus, it was likely not accurate and was influenced by self-reporting bias. Third, we used the remaining serum after routine testing in patients who were naturally infected; thus, obtaining the same time points of sera among patients was challenging. Finally, the reactivity of the SARS-CoV-2 antibody reagents could vary based on the type of SARS-CoV-2 antibody produced by natural infection and vaccination. Despite these limitations, the present study provides evidence of the association between the target antigen and immunoglobulin isotypes and their characteristics.

Ethics declaration

This study was approved by the Nagoya University Hospital Ethics Committee (identification number:2020-0095, 2021-0040).

Acknowledgments

The authors thank all the participants of this study. We thank Sysmex for technical support and for providing the CLEIA tests. We especially thank our laboratory staff who collected the sample/data.

Author Contributions

Conceptualization, R.K., J.K., and A.S.; methodology and investigation, J.K. and R.K.; data analysis, J.K., R.K., A.S.; Sample collection, J.K., R.W., K.G., and Y.O.; writing−original draft preparation, J.K.; writing—review and editing, R.K., A.S., R.W., K.G., and Y.O.; supervision, T.M. All the authors have read and agreed to the published version of the manuscript.

Data availability statement

The corresponding author had full access to all the data in the study and all authors shared final responsibility for the decision to submit for publication. The datasets generated during the current study are available from the corresponding author on reasonable request.

Funding

This publication was supported by a grant from Sysmex Corporation.

Competing interests

All reagents used for the analysis were provided by Sysmex Corporation. The Sysmex Corporation had no control over the interpretation, writing, or publication of this work.

References

1) World Health Organization: COVID-19 vaccine tracker and landscape.
<https://www.who.int/publications/m/item/draft-landscape-of-covid-19-candidate-vaccines>(Accessed August 5, 2023.)
2) Morinaga Y, Tani H, Terasaki Y, et al. Correlation of the commercial anti-SARS-CoV-2 receptor binding domain antibody test with the chemiluminescent reduction neutralizing test and possible detection of antibodies to emerging variants. Microbiol Spectr 2021; 9(3): e0056021.
3) Gruell H, Vanshylla K, Weber T, et al. Antibody-mediated neutralization of SARS-CoV-2. Immunity 2022; 55(6): 925-44.
4) Noval MG, Kaczmarek ME, Koide A, et al. Antibody isotype diversity against SARS-CoV-2 is associated with differential serum neutralization capacities. Sci Rep. 2021; 11(1): 5538.
5) Yang, Y, Yang M, Peng Y, et al. Longitudinal analysis of antibody dynamics in COVID-19 convalescents reveals neutralizing responses up to 16 months after infection. Nat Microbiol 2022; 7(3): 423-33.
6) Wang, Z, Muecksch F, Schaefer-Babajew D, et al. Naturally enhanced neutralizing breadth against SARS-CoV-2 one year after infection. Nature 2021; 595(7867): 426-31.
7) Borremans B, Gamble A, Prager KC, et al. Quantifying antibody kinetics and RNA detection during early-phase SARS-CoV-2 infection by time since symptom onset. elife 2020; 9: e60122.
https://doi.org/10.7554/eLife.60122
8) Anand SP, Prévost J, Nayrac M, et al. Longitudinal analysis of humoral immunity against SARS-CoV-2 Spike in convalescent individuals up to 8 months post-symptom onset. Cell Rep Med 2021; 2(6): 100290.
9) Noda K, Matsuda K, Yagishita S, et al. A novel highly quantitative and reproducible assay for the detection of anti-SARS-CoV-2 IgG and IgM antibodies. Sci Rep 2021; 11(1): 5198.
10) Crawford KHD, Dingens AS, Eguia R, et al. Dynamics of neutralizing antibody titers in the months after severe acute respiratory syndrome coronavirus 2 infection. J Infect Dis 2021; 223(2):197-205.
11) Bonifacio MA, Laterza R, Vinella A, et al. Correlation between In Vitro neutralization assay and serological tests for protective antibodies detection. Int J Mol Sci 2022; 23(17): 9566.
12) Muecksch F, Wise H, Templeton K, et al. Longitudinal variation in SARS-CoV-2 antibody levels and emergence of viral variants: a serological analysis. Lancet Microbe 2022; 3(7): e493-502.
13) Poon RW, Lu L, Fong CH, et al. Correlation between Commercial Anti-RBD IgG Titer and Neutralization Titer against SARS-CoV-2 Beta Variant. Diagnostics (Basel) 2021; 11(12): 2216.
14) Hale M, Netland J, Chen Y, et al. IgM antibodies derived from memory B cells are potent cross-variant neutralizers of SARS-CoV-2. J Exp Med 2022; 219(9): e20220849.
15) Pušnik J, König J, Mai K, et al. Persistent maintenance of intermediate memory B cells following SARS-CoV-2 infection and vaccination recall response. J Virol 2022; 96(15): e0076022.
16) Upasani V, Rodenhuis-Zybert I, Cantaert T. Antibody-independent functions of B cells during viral infections. PLoS Pathog 2021; 17(7): e1009708.
17) Fraussen J. IgM responses following SARS-CoV-2 vaccination: Insights into protective and pre-existing immunity. EBioMedicine 2022; 77: 103922.
18) Aranburu A, Ceccarelli S, Giorda E, et al. TLR ligation triggers somatic hypermutation in transitional B cells inducing the generation of IgM memory B cells. J Immunol 2010; 185(12): 7293-301.
19) Jeeva S, Kim KH, Shin CH, et al. An update on mRNA-based viral vaccines. Vaccines (Basel) 2021; 9(9): 965.
20) Tas JMJ, et al. Antibodies from primary humoral responses modulate the recruitment of naive B cells during secondary responses. Immunity. 2022; 55(10): 1856-1871.e6. 10.1016/j.immuni.2022.07.020
21) Ode H, et al. Molecular epidemiological features of SARS-CoV-2 in Japan, 2020-1. Virus Evol. 2022; 8(1): veac034. 10.1093/ve/veac034
22) Yafei LIU, Nakazaki Y, Arase H. Infectivity-enhancing antibodies against SARS-CoV-2. Translational and Regulatory Sciences 2022; 4(1): 1-4.
23) Liu Y, Soh WT, Kishikawa JI, et al. An infectivity-enhancing site on the SARS-CoV-2 spike protein targeted by antibodies. Cell 2021; 184(13): 3452-66.
24) Wang H, Yan D, Li Y, et al. Clinical and antibody characteristics reveal diverse signatures of severe and non-severe SARS-CoV-2 patients. Infect Dis Poverty 2022; 11(1): 15.